## 4. RESULTS AND DISCUSSION

To accomplish the projected aims and objectives the research work carried out has been discussed under three distinct headings:

**4.1 Chemical studies**

**4.2 Biological screening**

**4.3 Computational studies**

### 4.1 Chemical studies

In order to synthesis the compounds of our interest two different schemes (**general scheme 1-2)** were followed.

**4.1.1 General scheme 1** describes the synthesis of *N*-(4,5-di-(4-substituted phenyl)thaizol-2-yl)-2-(5-phenyl-2*H*-tetrazol-2-yl)acetamide (**186-224)** where substituted tetrazoles (**150-165**) were clubbed with 2-chloro-*N*-(4,5-di-(substitutedphenyl)thiazol-2-yl)acetamide.

**4.1.2 General scheme 2** describes the synthesis of (*Z*)-2-(2-((3-oxo-1,3 diphenylprop-1-en-1-yl)amino)ethyl) isoindoline-1,3-dione **(263-275)** and *N*-benzyl-1-(2-(1,3-dioxoisoindolin-2-yl)ethyl)piperidine-4-carboxamide derivatives (**288-297**).

#### 4.1.1 Synthesis of *N*-(4,5-di-(4-substitutedphenyl)thaizol-2-yl)-2-(5-phenyl-2*H*-tetrazol-2-yl)acetamide (186-224)

Under **general scheme 1** vicinal diaryl substituted tetrazole derivatives (**186-224)** were synthesized using compound (**150-164**). Synthesis of aryl-substituted tetrazoles (**150-164**) begins with the conversion of substituted benzaldehydes **(105-119**) to benzaldoximes, followed by their dehydration to benzonitriles. These benzonitriles undergo a 1,3-dipolar cycloaddition to yield 5-substituted-2*H*-tetrazoles **(150-164).**

For the preparation of the proposed compounds, vicinal diaryls (H, Cl, $OCH_3$) were synthesized using the Friedel-Crafts acylation reaction. The obtained ethanones were then brominated and cyclized using thiourea to form thiazole derivatives. These thiazole-2-amines were further modified through nucleophilic substitution and coupled with tetrazoles in the presence of potassium carbonate to obtain the final compounds, *N*-(4,5-di-(4-substitutedphenyl)thiazol-2-yl)-2-(5-phenyl-2*H*-tetrazol-2-yl)acetamide (**186-224**).

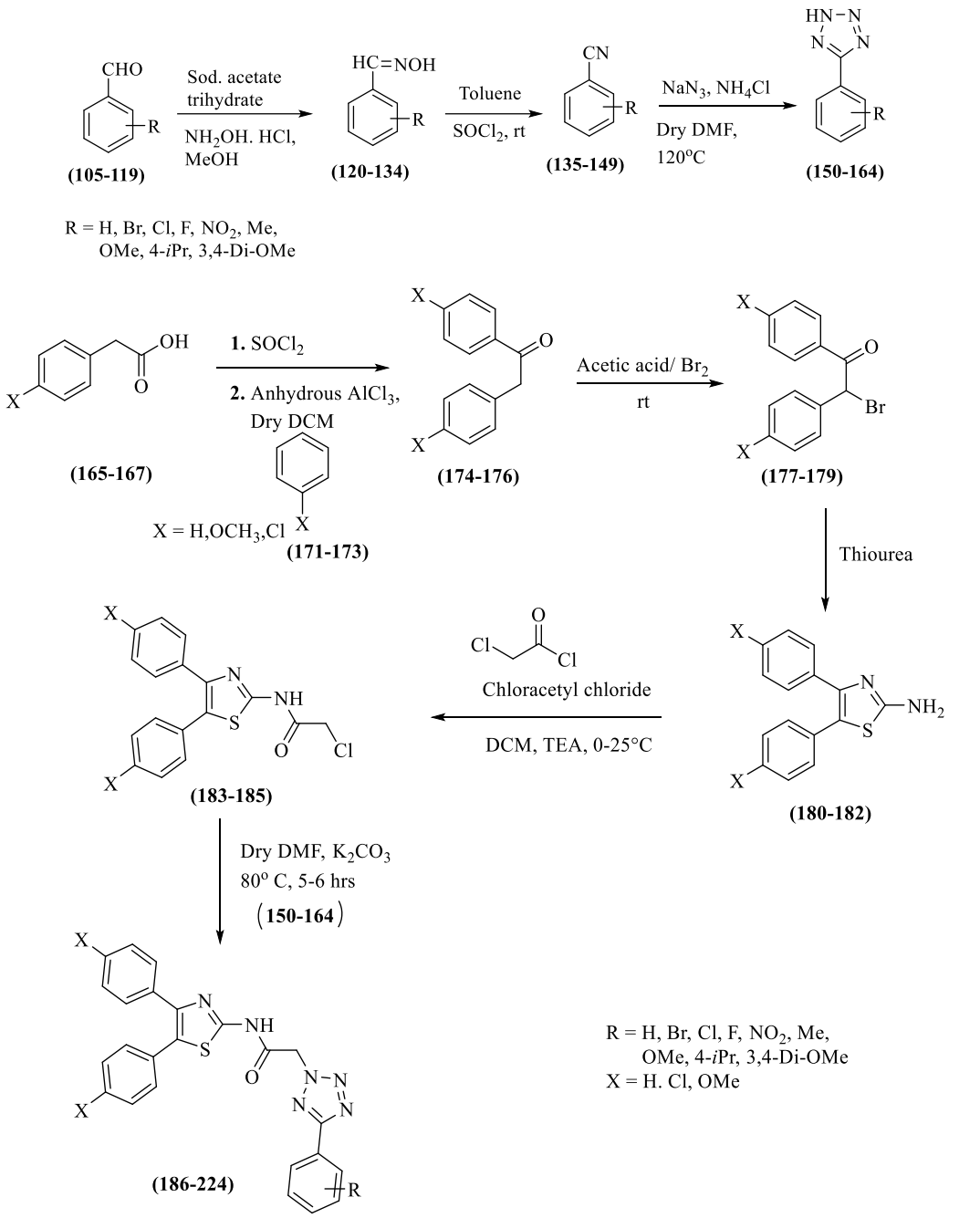


**General Scheme 1**: Synthesis of *N*-(4,5-di-(4-substitutedphenyl)thaizol-2-yl)-2-(5-phenyl-2*H*-tetrazol-2-yl) acetamide (**186-224)**

To execute the **general scheme 1**, substituted benzaldehydes, phenyl acetic acid, thiourea and chloracetyl chloride were procured directly from market. The steps followed for the synthesis of different intermediates of general scheme 1 has been discussed under following headings:

**4.1.1.1** Synthesis of substituted benzaldooximes (**120-134**)
**4.1.1.2** Synthesis of substituted benzonitriles **(135-149)**
**4.1.1.3** Synthesis of 5-substituted-2*H*-tetrazoles **(150-164)**
**4.1.1.4** Synthesis of substituted 1,2-di(4-subtituted phenyl)ethanones **(174-176)**

### 4.1.1.1 Synthesis of substituted benzaldoximes (120-134) [1-2]

Substituted benzaldoximes were synthesized when substituted benzaldehydes were condensed with sodium acetate trihydrate and hydroxylamine hydrochloride in methanol at temperature 60-80°C for 3-4 hrs. Synthesized compounds were characterized by IR spectra. The characteristic -OH stretching was observed in the range of 3300-3150 $cm^{-1}$ and C=N stretching was observed in the range of 1550-1690 $cm^{-1}$ (**Table 1**).

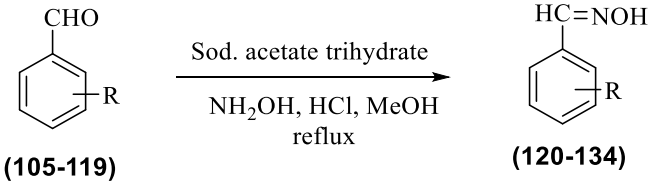


**(105-119)** **(120-134)**

**Scheme 1**

**Table 1**. IR spectral data of substituted benzoaldoximes **(120-134)**

| Comp | R | IR Peaks ($cm^{-1}$) |
|---|---|---|
| **120** | 3,4-Di-OMe | 3442 **(-OH stretch),** 1601 **(C=N stretch)**, 1265 (C-OMe) |
| **121** | 3-OH | 3600 **(-OH stretch),** 1620 (**C=N stretch)** |
| **122** | 4-OMe | 3300 **(-OH stretch)**, 1607 (**C=N stretch)** |
| **123** | 3-Cl | 3195**(-OH stretch)**, 1629 (**C=N stretch)** |
| **124** | 4-Br | 3299 **(-OH stretch)**, 1646 (**C=N stretch**) |
| **125** | 3-$NO_2$ | 3298 **(-OH stretch)**, 1617 (**C=N stretch)**, 1350 (asym. $NO_2$ stretch), C-N stretch (1209) |
| **126** | 4-Me | 3279 **(-OH stretch)**, 1605 (**C=N stretch)** |
| **127** | H | 3248 **(-OH stretch)**, 1601 (**C=N stretch)** |
| **128** | 3-Me | 3230 **(-OH stretch)**, 1525 (**C=N stretch)** |
| **129** | 3-OMe | 3356 **(-OH stretch)**, 1584 (**C=N stretch)** |
| **130** | 4-$N(CH_3)_2$ | 3300 **(-OH stretch)**, 1604 (**C=N stretch**), 1208 (C-N stretch), 1161 (CN bending) |
| **131** | 2-$NO_2$ | 3309 **(-OH stretch)**, 1605 (**C=N stretch)**, 1425 (asym. $NO_2$ stretch), 1209 (C-N stretch) |
| **132** | 3-Br | 3201 **(-OH stretch)**, 1629 (**C=N stretch)** |
| **133** | 4-*i*Pr | 3351 **(-OH stretch)**, 1611 (**C=N stretch)** |
| **134** | 4-F | 3191 **(-OH stretch)**, 1641 (**C=N stretch)** |

### 4.1.1.2 Synthesis of substituted benzonitriles (135-149)[3-6]

Substituted benzonitriles were synthesized on dehydration of substituted benzaldoximes using thionyl chloride and toluene. The substituted benzonitriles were characterized using IR spectra in which the characteristic peak of nitriles was observed between 2200-2300 $cm^{-1}$ (**Table 2**).

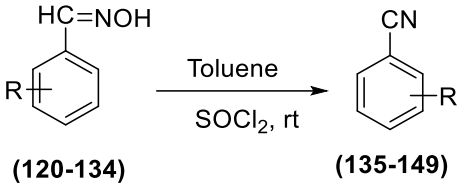


**Scheme 2**

**Table 2.** IR spectral data of substituted benzonitriles **(135-149)**

| Comp | R | IR peaks ($cm^{-1}$) |
|---|---|---|
| **135** | 3,4-Di-OMe | 2218 **(-CN stretching)**, 1268 **(-C-OMe)** |
| **136** | 3-OH | 2201 **(-CN stretching)** |
| **137** | 4-OMe | 2221 **(-CN stretching),** 1240 **(-C-OMe)** |
| **138** | 3-Cl | 2240 **(-CN stretching)** |
| **139** | 4-Br | 2265 **(-CN stretching)** |
| **140** | 3-$NO_2$ | 2229 **(-CN stretching)** |
| **141** | 4-Me | 2219 **(-CN stretching)** |
| **142** | H | 2300 **(-CN stretching)** |
| **143** | 3-Me | 2215 **(-CN stretching)** |
| **144** | 3-OMe | 2235 **(-CN stretching)** |
| **145** | 4-$N(CH_3)_2$ | 2284 **(-CN stretching)** |
| **146** | 2-$NO_2$ | 2238 **(-CN stretching)** |
| **147** | 3-Br | 2241 **(-CN stretching)** |
| **148** | 4-*i*Pr | 2237 **(-CN stretching)** |
| **149** | 4-F | 2248 **(-CN stretching)** |

### 4.1.1.3 Synthesis of 5-substituted-2*H*-tetrazole (150-164) [7–12]

The synthesized benzonitriles were reacted with sodium azide and ammonium chloride to yield 5-substituted-2*H*-tetrazole by under 1,3-dipolar cycloaddition reaction. The obtained compounds were characterized using IR spectra in which tetrazole peaks were observed (**Table 3**).

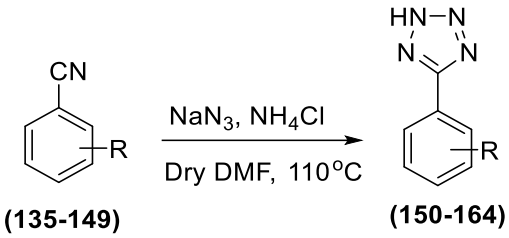


**(135-149)** **(150-164)**

**Scheme 3**

**Table 3**. IR spectral data of 5-substituted-2*H*-tetrazole **(150-164)**

| Comp | R | IR peaks ($cm^{-1}$) |
|---|---|---|
| **150** | 3,4-Di-OMe | 3420 **(-NH stretching**), 1234, 1144 **(tetrazole ring)** |
| **151** | 3-OH | 3389 **(-NH stretching),** 1284, 1168, 1054 **(tetrazole ring)** |
| **152** | 4-OMe | 3428 **(-NH stretching),** 1258, 1195, 1068 **(tetrazole ring)** |
| **153** | 3-Cl | 3449 **(-NH stretching),** 1238, 1149, 1094 **(tetrazole ring)** |
| **154** | 4-Br | 3109 **(-NH stretching),** 1267, 1136, 1102 **(tetrazole ring)** |
| **155** | 3-$NO_2$ | 3379 **(-NH stretching),** 1264, 1158, 1060 **(tetrazole ring)**, 1567 (**$NO_2$ strech)** |
| **156** | 4-Me | 3439 **(-NH stretching),** 1269, 1171, 1069 **(tetrazole ring)** |
| **157** | H | 3440 **(-NH stretching),** 1254, 1109, 1025**(tetrazole ring)** |
| **158** | 3-Me | 3429 **(-NH stretching),** 1298, 1138, 1023 **(tetrazole ring)** |
| **159** | 3-OMe | 3451 **(-NH stretching),** 1247, 1159, 1032**(tetrazole ring)** |
| **160** | 4-$N(CH_3)_2$ | 3321**(-NH stretching),** 1648 **(C=N stretch),** 1254, 1108 **(tetrazole ring)** |
| **161** | 2-$NO_2$ | 3465 **(-NH stretching),** 1239, 1143, 1009 **(tetrazole ring)** |
| **162** | 3-Br | 3421 **(-NH stretching),** 1275, 1151, 1098 **(tetrazole ring)** |
| **163** | 4-*i*Pr | 3149 **(-NH stretching),** 1246, 1129, 1061 **(tetrazole ring)** |
| **164** | 4-F | 3431 **(-NH stretching),** 1256, 1125, 1087 **(tetrazole ring)** |

### 4.1.1.4 Synthesis of 1,2-di(4-subtitutedphenyl)ethanones (174-176)

To synthesis 1,2-di(4-substitutedphenyl)ethanones two-step reaction was followed as depicted in scheme 4. In first step substituted phenyl acetic acid was reacted with thionyl chloride to obtain substituted phenyl acetyl chlorides. Subsequently, in second step Friedel-Craft acylation was followed when substituted phenyl acetyl chlorides were reacted with substituted benzene in the presence of anhydrous ammonium chloride to yield 1,2-di(4-subtitutedphenyl)ethanones. The obtained compounds were characterized using IR spectra in which characteristic peak of carbonyl was observed at 1675 $cm^{-1}$, 1681 and 1688 $cm^{-1}$.

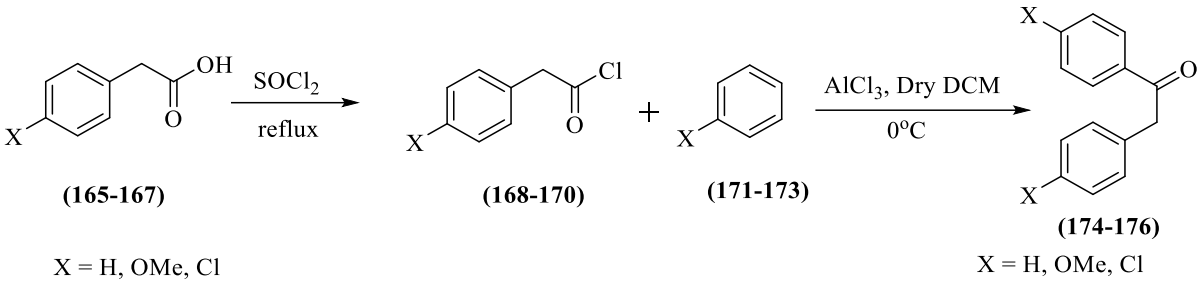


**(165-167)**

X = H, OMe, Cl

**(168-170)**

**(171-173)**

**(174-176)**

X = H, OMe, Cl

**Scheme 4**

### 4.1.1.5 Synthesis of 2-bromo-1, 2-di(4-substitutedphenyl)ethanones (177-179)

In presence of bromine and acetic acid, 2-bromo-1,2-di(4-substitutedphenyl)ethanones were synthesized, which were characterized by the IR spectra. In the IR spectra carbonyl stretching will shift a bit due to the presence of bromine towards 1664 $cm^{-1}$, 1677 $cm^{-1}$ and 1683 $cm^{-1}$.

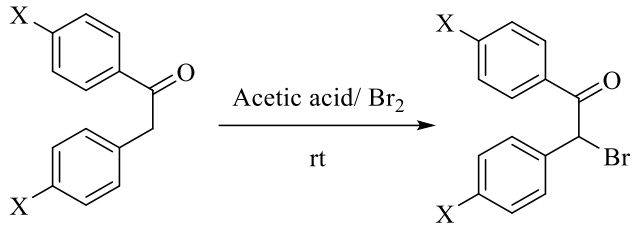


**(174-176)**

X = H, OMe, Cl

**(177-179)**

X = H, OMe, Cl

**Scheme 5**

### 4.1.1.6 Synthesis of 4,5-di(substitutedphenyl)thiazol-2-ylamine (180-182)

2-Bromo-1,2-di(4-substitutedphenyl)ethanones on reaction with thiourea in the presence of methanol resulted into synthesis of 4,5-di(substitutedphenyl)thiazol-2-ylamine and characterized by using IR spectra. In IR spectra -NH stretching peak was the characteristic peak for the synthesized compounds (**Table 4**).

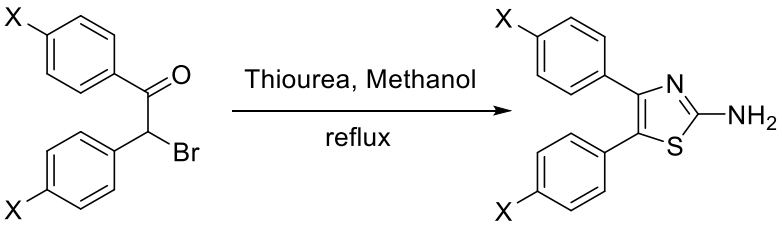


**(177-179)**

X = H, OMe, Cl

**(180-182)**

X = H, OMe, Cl

**Scheme 6**

**Table 4** IR spectral data of 4,5-di(substitutedphenyl)thiazol-2-ylamine **(180-182)**

| Compound | X | IR Spectra ($cm^{-1}$) |
|---|---|---|
| **180** | H | 3400 **(-NH stretching),** 3201, 1610 |
| **181** | OMe | 3428 **(-NH stretching),** 3198, 1620 |
| **182** | Cl | 3445 **(-NH stretching),** 3219, 1635 |

### 4.1.1.7 Synthesis of 2-chloro-*N*-(4,5-di-(substitutedphenyl)thiazol-2-yl)acetamide (183-185)

4,5-Di-(substitutedphenyl)thiazol-2-ylamine reacted with chloroacetyl chloride in presence of solvent DCM and TEA resulted into synthesis of 2-chloro-*N*-(4,5-di-(substitutedphenyl)thiazol-2-yl)acetamide. The obtained compound was characterized using IR spectra. The characteristic peak of amide was observed at 1618 $cm^{-1}$ for compound **(183**) along with the carbonyl peak at 1215 $cm^{-1}$. For compound (**184**) and (**185)** amide peak was observed at 1630 and 1645 $cm^{-1}$ along with the carbonyl peak at 1221 and 1238 $cm^{-1}$.

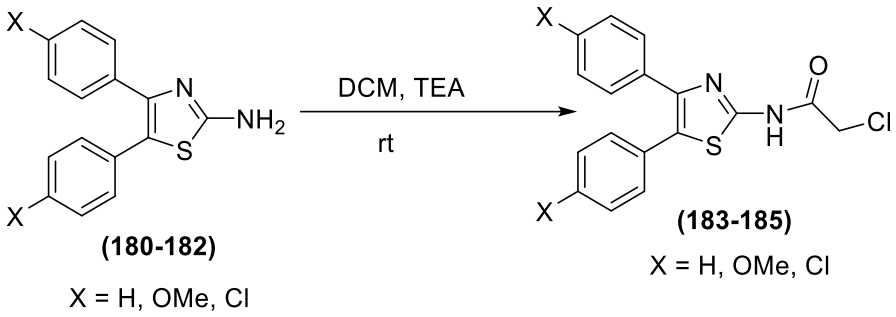


**Scheme 7**

### 4.1.1.8 Synthesis of *N*-4,5-di(substituted phenyl)thiazol-2-yl)-2-(5-(substituted)-2*H*-tetrazol-2-yl)acetamide (186-224)

2-Chloro-*N*-(4,5-di-(substitutedphenyl)thiazol-2-yl)acetamide was reacted with 5-substituted tetrazole in the presence of potassium carbonate and DMF to get *N*-4,5-di(substitutedphenyl)thiazol-2-yl)-2-(5-(substituted)-2*H*-tetrazol-2-yl)acetamide.

From the previous studies reported by Mahesh *et al.* [10] from our lab it was revealed that in tetrazole, alkylation was progressed at 2nd position of nitrogen. The synthesized compounds were characterized using IR, Mass and NMR spectroscopy.

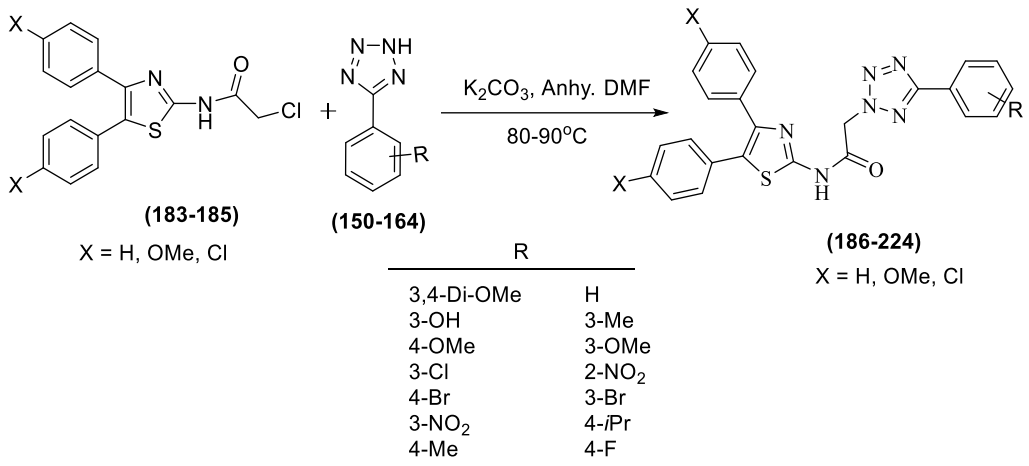


**Scheme 8**

In the IR spectrum of the synthesized compound (**186**), C=O stretching of amide was observed at 1695 $cm^{-1}$ and peaks for tetrazole were observed at 1284 and 754 $cm^{-1}$. Its PMR spectra showed signals for one aromatic proton at δ 7.65 (d, *J* = 7.7 Hz, $1H_d$) in aromatic ring, a multiplate was observed for two protons at δ 7.49 – 7.46 (m, $2H_{m,n}$), another multiplate signal was observed at δ 7.44 (s, $1H_j$), and δ 7.34-7.32 (m, $3H_{i,o,e}$) for three aromatic protons. Other multiplate signals of aromatic protons were observed at δ 7.30 (d, *J* = 5.8 Hz, $6H_{a,b,c,f,g,i}$) and 6.92 (dd, *J* = 7.9, 2.1 Hz, $1H_{h,}$). A singlet peak of aliphatic protons of spacer was observed at 4.86 (s, 2H) respectively. Mass spectrum of this compound (**186**) showed molecular ion peak at m/z 455 $(M+1)^+$.

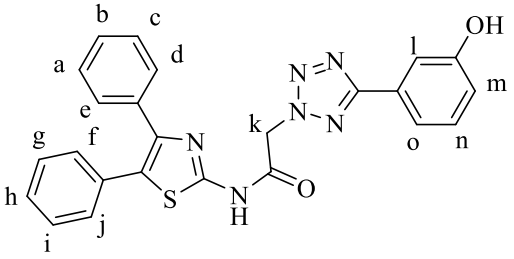


**(186)**

In the IR spectrum of synthesized compound (**187**), C=O stretching of amide was observed at 1703 $cm^{-1}$ and peaks for tetrazole were observed at 1292 and 758 $cm^{-1}$. Its PMR spectra showed NH peak at δ 11.83 (s, 1H), a multiplate at δ 8.07 – 8.03 (m, $2H_{d,j}$) in aromatic ring for two protons, another multiplate was observed for two protons at δ 7.53 – 7.48 (m, $2H_{m,n}$), a doublet over doublet signal was observed at δ 7.34 (dd, J = 4.2, 2.4 Hz, $3H_{b,c,e}$), and δ 7.32 – 7.27 (m, $5H_{f,g,I,l,o}$) for five aromatic protons. Other multiplate signals of aromatic protons were observed at δ 7.01-6.97 (m,

$2H_{a,h}$). A singlet peak of aliphatic protons of spacer was observed at 4.76 (s, $2H_k$) and a singlet of methoxy group was seen at 3.86 (s,$3H_p$) respectively. Mass spectrum of this compound (**187**) showed molecular ion peak at m/z 469.4 $(M+1)^+$.

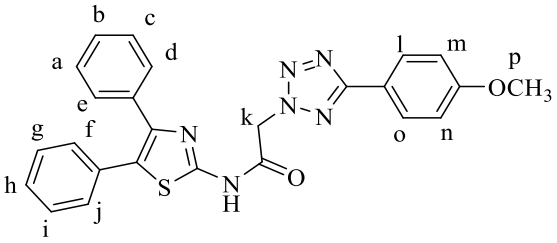


**(187)**

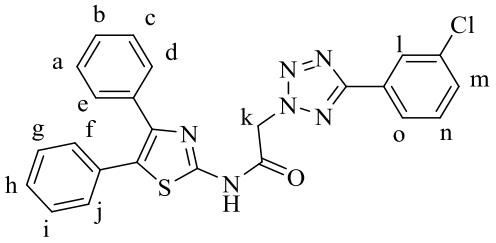


**(188)**

In the IR spectrum of synthesized compound (**188**), C=O stretching of amide was observed at 1697 $cm^{-1}$ and peaks for tetrazole were observed at 1278 and 774 $cm^{-1}$. Its PMR spectra showed NH peak at δ 12.21 (s, 1H), a doublet at δ 8.12 (d, J = 1.8 Hz, $1H_l$) in aromatic ring for one proton, another doublet over triplet was observed for one proton at δ 8.01 (dt, J = 7.1, 1.6 Hz, $1H_m$), a doublet over doublet signal was observed at δ 7.53 (dd, J = 6.6, 3.0 Hz, $2H_{d,j}$), and a multiplate at δ 7.48 – 7.42 (m, $2H_{e,f}$) for two aromatic protons. Other multiplate signals of aromatic protons were observed at δ 7.41 – 7.36 (m, $3H_{a,b,c}$), 7.36 (s, $2H_{n.o}$) and 7.25 (d, J = 4.8 Hz, $3H_{g,h,i}$). A singlet peak of aliphatic protons of spacer was observed at 4.65 (s, $2H_k$). Mass spectrum of this compound (**188**) showed molecular ion peak at m/z 473 $(M)^+$ and isotopic peak at 475.2 $(M+2)^+$.

In the IR spectrum of synthesized compound (**189**), C=O stretching of amide was observed at 1697 $cm^{-1}$ and peaks for tetrazole were observed at 1278, 1084 and 774 $cm^{-1}$. Its PMR spectra showed signals for one aromatic proton at δ 8.30 (t, $1H_d$) in aromatic ring, a multiplate was observed for one proton at δ 8.10-8.05 (m, $1H_j$), another multiplate signal was observed at δ 7.63-7.57 (m, $2H_{m,\ n}$), and δ 7.52-7.48 (m, $2H_{i,}$ o) for four aromatic protons. Other multiplate signals of aromatic protons were observed at δ 7.39-7.33 (m, $4H_{a,\ b,\ c,e}$) and δ 7.32 (s, $4H_{f,\ g,\ h,\ i}$). A singlet peak of aliphatic protons of spacer was observed at 4.87 (s, 2H) respectively. Mass spectrum of this compound (**189**) showed molecular ion peak at m/z 516.9 $(M)^+$.

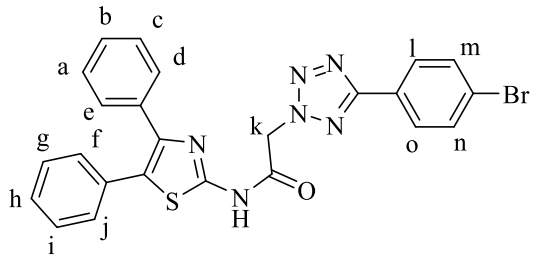

**(189)**

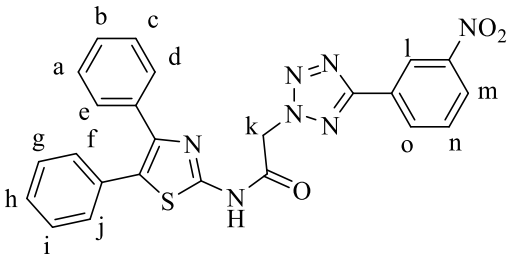

**(190)**

IR spectra of synthesized compound (**190)** offered NH stretching at 3297 $cm^{-1}$ and C=O stretching peak of amide at 1699 $cm^{-1}$. Its PMR spectra offered a multiplate for one aromatic proton at δ 8.99-8.93 (m, $1H_l$), for another proton a doublet was offered at 8.47 (d, $1H_d$), and a doublet over doublet was offered at 8.34 (dd, $1H_j$). For the tetrazole containing benzyl ring protons a triplet peak was observed at 7.69 (t, $1H_m$) for one proton and a multiplate was observed from 7.57-7.50 (m, $2H_{n,o}$) for two protons. For others protons of vicinal diaryl moiety a doublet over doublet peak and a multiplate was observed at 7.39-7.33 (dd, $8H_{a,\ b.c.e,f,\ g,h,i}$). For the aliphatic linker the PMR spectra shows a singlet peak for two protons at 4.65 (s, $2H_k$). Mass spectrum of compound **(190)** showed molecular ion peak at m/z 484.4$(M)^+$.

IR spectra of synthesized compound (**191)** offered NH stretching at 3251 $cm^{-1}$ and C=O stretching at 1704 $cm^{-1}$. Its PMR spectra offered a doublet for two aromatic protons of vicinal diaryl moiety at 8.02 (d, $2H_{d,\ j}$), and a doublet over doublet for two protons of tetrazole containing benzyl moiety at 7.49 (dd, $2H_{m,n}$). For other aromatic protons of a multiplate peak was observed at 7.37-7.27 (m, $10H_{a,b,c,e,f,g,h,i,l.o}$). The peak of aliphatic protons of linker was observed at 4.92 (d, $2H_k$) and the most shield peak of the methyl group was observed at 2.42 (s, $3H_p$). Mass spectrum of compound (**191**) showed molecular ion peak at 453.2 $(M)^+$.

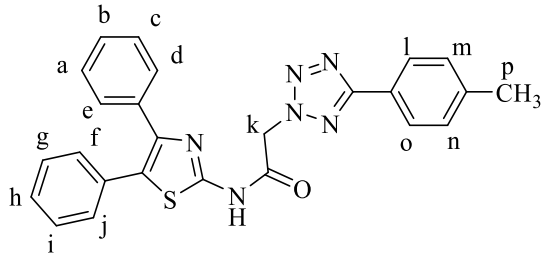

**(191)**

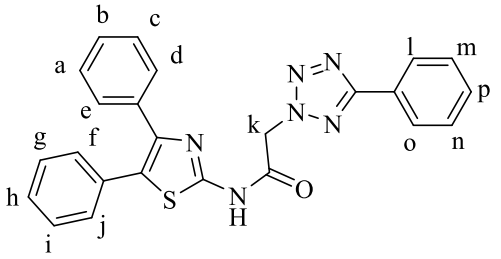

**(192)**

IR spectra of synthesized compound (**192)** showed NH stretching at 3187 $cm^{-1}$ and carbonyl stretching at 1687 $cm^{-1}$. The PMR spectra of compound showed a doublet over doublet peak for one proton at 8.11 (dd, $1H_d$) and a multiplate for three protons at 7.56-7.49 (m, $3H_{j,l,o}$) and a triplet for two protons at 7.46 (t, $2H_{e,f}$). Other peaks of aromatic protons were observed as a multiplate at 7.37-7.24 (m, $9H_{a,\ b,\ c,\ g,h,i,m,n,p}$). The protons of linker in the aliphatic region were observed as a multiplate at 4.53(m, $2H_k$) for two protons. Mass spectrum of compound (**192**) showed molecular ion peak at 437.0 $(M)^-$.

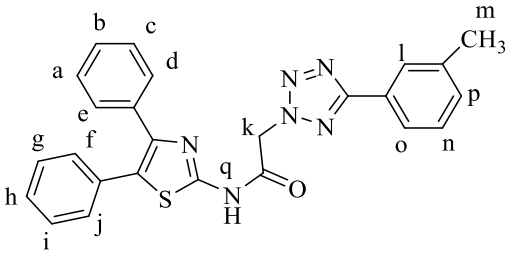


**(193)**

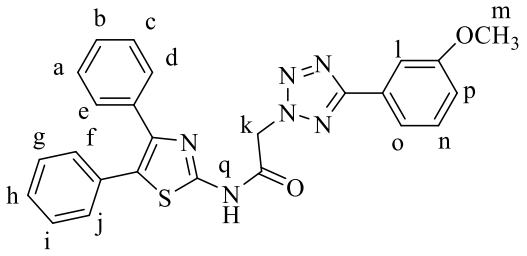


**(194)**

IR spectra of synthesized compound (**193)** offered NH stretching at 3326 $cm^{-1}$ and C=O stretching at 1697 $cm^{-1}$. Its PMR spectra showed a broad singlet of NH at 11.94 (s, $1H_q$) along with this a multiplate was observed at 7.97-7.88 (m, $2H_{d,\ j}$) for two protons and an another multiplate observed for two protons at 7.54-7.49 (m, $2H_{i,p}$). For other aromatic protons of compound, multiplate peaks were observed at 7.40-7.33 (m, $4H_{e,f.n,o}$) and 7.33-7.27 (m, $6H_{a,b,c,g,h,i}$). The peak of aliphatic protons of linker was observed at 4.76 (d, $2H_k$) and the most shield peak of the methyl group was observed at 2.42 (s, $3H_p$). Mass spectrum of compound (**193**) showed molecular ion peak at 453.4 $(M)^+$.

IR spectra of synthesized compound (**194)** offered NH stretching at 3234 $cm^{-1}$ and C=O stretching at 1703 $cm^{-1}$. Its PMR spectra showed a broad singlet of NH at 11.39 (s, $1H_q$) along with this a multiplate was observed at 8.11-8.02 (m, $2H_{d,\ j}$) for two protons and an another multiplate observed for two protons at 7.54-7.46 (m, $2H_{i,p}$). For other aromatic protons of compound, multiplate peaks were observed at 7.38-7.27 (m, $8H_{\ b,c,e,f.g,i,n,o}$) and 7.03-6.95 (m, $2H_{a,h}$). The peak of aliphatic protons of linker was observed at 4.90 (s, $2H_k$) and at 2.42 (s, $3H_p$) protons of methoxy group shows a singlet peak. $^{13}C$ NMR shows a carbonyl peak at δ 165.58 and aromatic carbon peaks at 162.40,

161.41, 157.16, 143.71, 134.29, 131.01, 129.35, 129.10, 129.05, 128.87, 128.79, 128.49, 128.19, 119.39 and 114.25. The aliphatic peaks observed at 55.33, 53.37. Mass spectrum of compound (**194)** showed molecular ion peak at m/z 469.5 $(M)^+$.

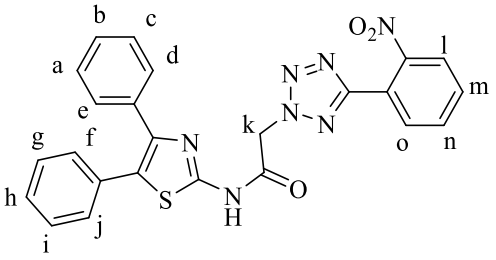


**(195)**

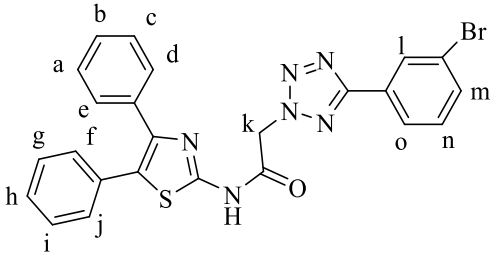


**(196)**

IR spectra of synthesized compound **(195)** offered NH stretching at 3197 $cm^{-1}$ and C=O stretching peak of amide at 1701 $cm^{-1}$. Its PMR spectra offered a doublet over doublet for one aromatic proton at δ 7.97 (dd, $1H_l$), for another proton a doublet was offered at 7.89 (dd, $1H_d$), and a triplet over doublet was offered at 7.71 (td, $1H_j$) and at 7.65 (td, $J$ = 7.8, 1.5 Hz, $1H_m$). For the tetrazole containing benzyl ring protons a doublet over triplet peak was observed at 7.53 (dt, $J$ = 9.1, 4.2 Hz, $2H_{n,o}$) and at 7.37 (dt, $3H_{e,f,g}$) for three protons and for others protons of vicinal diaryl moiety a multiplate was observed at 7.35-7.28( m, $5H_{a,b.c,,h,i}$). For the aliphatic linker the PMR spectra shows a singlet peak for two protons at 4.65(s, $2H_k$). The mass spectrum of compound (**195**) showed molecular ion peak at m/z 484.1 $(M)^+$.

IR spectra of synthesized compound (**196)** offered NH stretching at 3317 $cm^{-1}$ and C=O stretching peak of amide at 1698 $cm^{-1}$. Its PMR spectra showed a triplet peak at 8.29 t, $J$ = 1.7 Hz, $1H_l$) for one proton having bromine group to its adjacent carbon atom and another multiplate peak was observed at 8.09-8.02 (m, $1H_m$), for other protons a multiplate was offered at 7.63-7.58 (m, $1H_d$), and at 7.53-7.47 (m, $2H_{j,\ o}$). Other aromatic protons of compound showed multiplate at 7.38-7.33 (m, $4H_{e,f,i,n.}$) for four protons and at 7.33-7.29 (m, $5H_{a,b,c,g,h}$) for five protons. For the aliphatic linker the PMR spectra showed a singlet peak for two protons at 4.75 (s, $2H_k$). The mass spectrum of compound **(196**) showed molecular ion peak at m/z 517.4 $(M)^+$, and an isotopic peak at m/z 519.3 $(M+2)^+$.

IR spectra of synthesized compound (**197)** offered NH stretching at 3317 $cm^{-1}$ and C=O stretching peak of amide at 1698 $cm^{-1}$. Its PMR spectra showed a doublet peak

at 8.02 (d, *J* = 8.2 Hz, $2H_{d,j}$) for two protons and a multiplate peak at 7.56-7.46 (m,$3H_{l,o,e}$). Another peaks for aromatic protons were observed as doublet over doublet for five protons at 7.34 (dd, *J* = 8.2, 4.6 Hz, 5H $c_{,f,g,m,n,}$) and a doublet for four protons at 7.25 (d, *J* = 10.5 Hz, $4H_{a,b,h,i}$). The aliphatic proton peaks of this compound observed as doublet at 4.60 (d, *J* = 27.0 Hz, $2H_k$), multiplate at 3.01-2.88 (m, $1H_r$) and a doublet over doublet at 1.26 (dd, *J* = 11.9, 7.0 Hz, $6H_{p,q}$) for six protons. $^{13}C$ NMR spectra showed carbonyl peak at 165.69 and aromatic peaks were observed at 162.42, 157.20, 151.61, 143.69, 134.30, 131.03, 129.46, 129.34, 129.09, 129.02, 128.85, 128.74, 128.59, 128.42, 128.19, 128.15, 127.97, 126.98, 126.94 and 124.38. The aliphatic carbon peak were observed at 53.32, 34.09 and 23.79. The mass spectrum of compound **(197)** showed molecular ion peak at m/z 481.2 $(M)^+$.

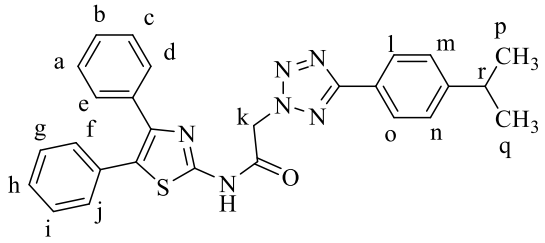

(**197)**

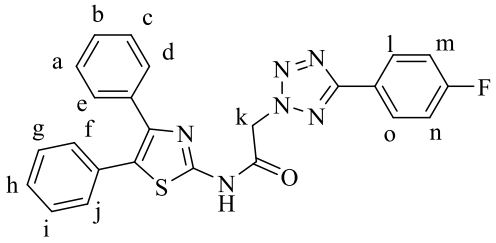

**(198)**

IR spectra of synthesized compound (**198)** showed C=O stretching peak of amide at 1689 $cm^{-1}$. Its PMR spectra shows a multiplate peak at 8.15-8.05 (m, $2H_{d,j}$) for two protons and a multiplate peak at 7.57-7.47 (m,$3H_{m,n,l}$). Another peaks for aromatic protons were observed as multiplate at 7.40-7.34 (m, $3H_{o,e,f}$) for three protons, as doublet for four protons at 7.25 (d, *J* = 9.5 Hz, $4H_{b,c,h,i}$) and a doublet over doublet at 7.15 (dd, *J* = 19.1, 10.4 Hz, $2H_{a,g}$). The aliphatic protons were observed as a singlet at 4.58 (s, $2H_k$). The mass spectrum of compound (**198**) shows molecular ion peak at m/z 455.0 (M-1) and 457.0 $(M+1)^+$.

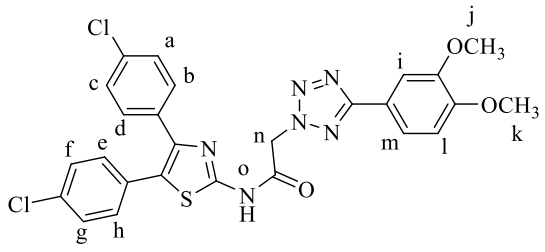

(**199)**

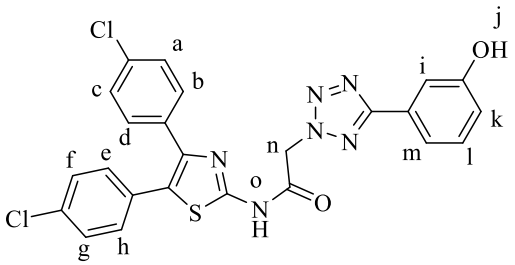

**(200)**

IR spectrum of synthesized compound (**199)** showed NH stretching at 3208 $cm^{-1}$ and carbonyl stretching at 1711 $cm^{-1}$ along with the C-O peak at 1249 $cm^{-1}$. Its PMR spectra showed a broad singlet peak for NH at δ 10.45 (s, $1H_o$), the spectra has shown a doublet over doublet peak at 7.77 (dd, $J$ = 8.4, 1.9 Hz, $1H_c$) and a doublet at 7.67 (d, $J$ = 1.9 Hz, $1H_f$). Another aromatic protons of the compound were observed at 7.38 – 7.34 (m, $2H_{a,g}$), 7.30 (dd, $J$ = 9.3, 2.6 Hz, $4H_{b,d,e,h}$), 7.25 – 7.21 (m, $2H_{i,l}$) and 6.97 (d, $J$ = 8.4 Hz, $1H_m$). The aliphatic protons of the spacer were observed as a singlet at 5.32 (s, $2H_n$) and the six methoxy protons were observed as a doublet at 3.96 (d, $J$ = 10.9 Hz, $6H_{j,k}$). The mass spectrum of compound (**199**) showed molecular ion peak at m/z 567.0$(M)^-$ and isotopic peak at 569.1 $(M+2)^+$.

IR spectrum of synthesized compound (**200)** showed an OH stretching at 3600 $cm^{-1}$ NH stretching at 3157 $cm^{-1}$ and carbonyl stretching at 1696 $cm^{-1}$ along with the C-O peak at 1249 $cm^{-1}$. Its PMR spectra has shown a doublet peak at δ 7.67 (dd, $J$ = 7.7 Hz, $1H_c$) and another peak at 7.53 (d, $J$ = 6.1 Hz, $1H_f$). Another aromatic protons of the compound were observed at 7.36 (d , $J$ = 8.6 Hz, $2H_{a,g}$), 7.34-7.30 (m, $2H_{b,d,}$), 7.30 – 7.26 (m, $3H_{e,h,i,}$), 7.24-7.18 (m, $2H_{k,m}$ and 6.93 (dd, $J$ = 8.1, 1.9 Hz, $1H_l$). The aliphatic protons of the spacer were observed as a singlet at 5.27 (s, $2H_n$). The mass spectrum of compound (**200**) showed molecular ion peak at m/z 523.0$(M)^+$ and isotopic peak at 525.0 $(M+2)^+$.

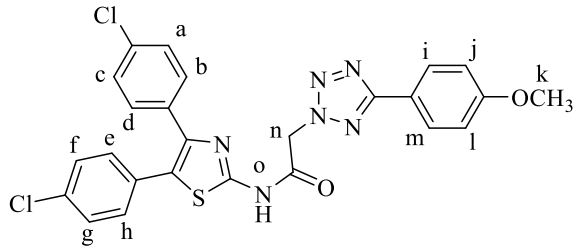


**(201)**

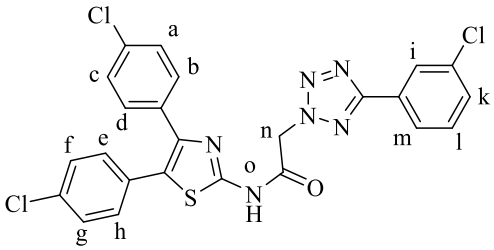


**(202)**

IR spectrum of synthesized compound **(201)** showed carbonyl stretching at 1696 $cm^{-1}$ along with the C-O peak at 1286 $cm^{-1}$. Its PMR spectra has showed multiplate peak at 8.16-8.06 (m, $2H_{c,f}$) and another peak at 7.38-7.33 (m, $2H_{a,g}$). Another aromatic protons of the compound were observed at 7.33 – 7.29 (m, $2H_{d,e}$), 7.27 (d, $J$ = 2.1 Hz, $1H_b$), 7.25 (t, $J$ = 2.3Hz, $2H_{j,l}$), 7.23 (d, $J$ = 1.9 Hz, $1H_h$), and 7.05-7.00 (m, $2H_{i,m}$). The aliphatic protons of the spacer were observed as a singlet at 5.45(s, $2H_n$) and the three methoxy protons were observed as a singlet at 3.88 (s, $3H_k$). The mass spectrum of

compound (**201**) showed molecular ion peak at m/z at 539.1 $(M+2)^+$.

IR spectrum of synthesized compound (**202)** showed NH stretching at 3317 $cm^{-1}$ and carbonyl stretching at 1699 $cm^{-1}$ along with the C-O peak at 1289 $cm^{-1}$. Its PMR spectra showed NH peak at δ 10.43 (s, 1H), the spectra have showed a doublet peak at 8.17 (d, *J* = 1.8 Hz, $1H_{c,}$) and another peak at 8.06 (dt, *J* = 7.2, 1.6 Hz, $1H_f$). Another aromatic protons of the compound were observed at 7.48 (ddt, *J* = 16.6, 15.4, 5.0 Hz, $2H_{i,k}$), 7.41 – 7.35 (m, $2H_{l.m}$), 7.33 – 7.27 (m, $4H_{b,d,e,h}$), 7.25 – 7.21 (m, $2H_{a,g}$). The aliphatic protons of the spacer were observed as a singlet at 5.30 (d, *J* = 21.0 Hz, $2H_n$). The mass spectrum of compound (**202**) showed molecular ion peak at m/z 540.9$(M)^+$ and isotopic peak at 542.8 $(M+2)^+$.

IR spectrum of synthesized compound (**203)** showed NH stretching at 3163 $cm^{-1}$ and carbonyl stretching at 1698 $cm^{-1}$ along with the C-O peak at 1288 $cm^{-1}$. Its PMR spectra has shown a singlet peak at 8.39 (s, $1H_{c,}$) and another peak at 8.12 – 8.01 (m, $2H_{j,l}$). Another aromatic protons of the compound were observed 7.70 – 7.61 (m, $2H_{i,m}$), 7.39 – 7.33 (m, $2H_{b.h}$), 7.31 (dd, *J* = 11.1, 4.5 Hz, $2H_{e,d}$), 7.27 (t, *J* = 2.5 Hz, $1H_f$), 7.23 (d, *J* = 2.0 Hz, $2H_{a,g}$). The aliphatic protons of the spacer were observed as a singlet at 5.56 (s, $2H_n$). The mass spectrum of compound (**203**) showed molecular ion peak at m/z 587.2 $(M+1)^+$ and isotopic peak at 589.2 $(M+2)^+$.

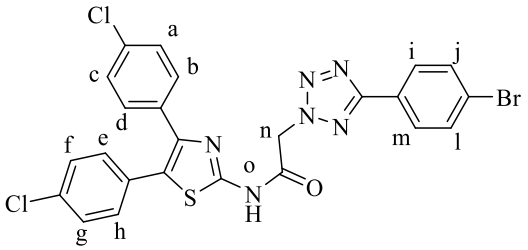


**(203)**

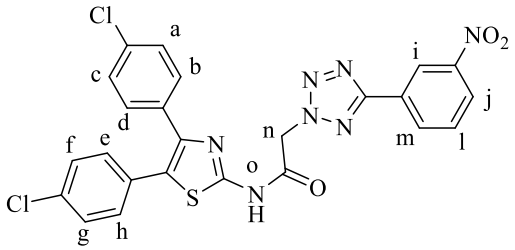


**(204)**

IR spectrum of synthesized compound (**204)** showed NH stretching at 3299 $cm^{-1}$ and carbonyl stretching at 1699 $cm^{-1}$ along with the C-O peak at 1289 $cm^{-1}$. Its PMR spectra showed NH peak at δ 10.55 (s, $1H_o$), its spectra has shown multiplate peak at 9.05 – 8.99 (m, $1H_c$) and another peak at 8.58 – 8.47 (m, $1H_f$). Another aromatic protons of the compound were observed 8.37 (ddd, *J* = 8.3, 2.3, 1.0 Hz, $1H_i$), 7.73 (t, *J* = 8.0 Hz, $1H_j$), 7.42 – 7.36 (m, $2H_{l,m}$), 7.35 – 7.27 (m, $4H_{b,d,g,h}$), 7.25 – 7.21 (m, $2H_{a,g}$). The aliphatic protons of the spacer were observed as a singlet at 5.31 (s, $2H_n$). Its $^{13}C$ spectra showed carbonyl peak at 164.11 and the aromatic carbon peaks were

observed at 148.65, 132.63, 132.18, 130.56, 130.14, 129.36, 129.28, 128.39, 125.29 and 122.06. The aliphatic carbon peaks were observed at 54.17 and 52.72. The mass spectrum of compound (**204**) showed molecular ion peak at m/z 554.0 $(M+2)^+$.

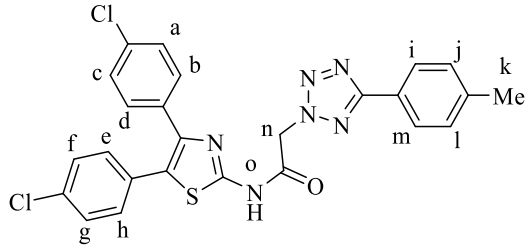


**(205)**

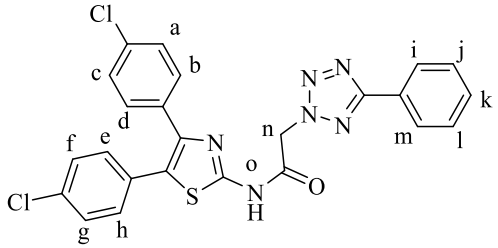


**(206)**

IR spectrum of synthesized compound (**205)** showed carbonyl stretching at 1698 $cm^{-1}$ along with the C-O peak at 1289 $cm^{-1}$. Its PMR spectra has shown multiplate peak at δ 8.08 (d, *J* = 8.2 Hz, $2H_{c,f}$) and another peak at 7.55 – 7.48 (m, $1H_b$). Another aromatic protons of the compound were observed 7.41 – 7.36 (m, $2H_{d,e}$), 7.33 (d, *J* = 10.2 Hz, $3H_{a,g,h}$), 7.29 (dd, *J* = 4.9, 2.1 Hz, $2H_{j,l}$) and 7.24 (d, *J* = 3.7 Hz, $2H_{i,m}$). The aliphatic protons of the spacer were observed as a singlet at 5.56 (s, $2H_n$) and another singlet was observed at 2.44 (s, $3H_k$) for methyl protons. The mass spectrum of compound (**205**) showed molecular ion peak at m/z 523.3 $(M+2)^+$.

IR spectrum of synthesized compound (**206)** showed carbonyl stretching at 1686 $cm^{-1}$ along with the C-O peak at 1288 $cm^{-1}$. Its PMR spectra showed NH peak at δ 10.49 (s, $1H_o$), it has shown multiplate peak at δ 8.20-8.13 (m, $2H_{c,f}$) and another peak at 7.50 (dd, *J* = 9.3, 6.1 Hz, $3H_{a,b.d}$). Another aromatic protons of the compound was observed 7.38 (dd, *J* = 11.6, 5.0 Hz, $2H_{i,m}$), 7.30 (dd, *J* = 8.3, 1.5 Hz, $3H_{j,k,l}$), 7.27 (s, $1H_e$) and 7.24 – 7.20 (m, $2H_{g,h}$). The aliphatic protons of the spacer were observed as a singlet at 5.32 (s, $2H_n$). $^{13}C$ spectra showed carbonyl peak at 166.12 and aromatic carbons peak at 161.91, 155.99, 143.27, 134.61, 134.53, 132.29, 130.84, 130.63, 130.11, 129.44, 129.28, 129.06, 128.97, 127.27, 127.05, 126.52. The aliphatic carbon peak was observed at 54.28. The mass spectrum of compound **(206)** showed molecular ion peak at m/z 508.9 $(M+1)^+$.

IR spectrum of synthesized compound (**207)** showed NH stretching at 3317 $cm^{-1}$ and carbonyl stretching at 1700 $cm^{-1}$ along with the C-O peak at 1288 $cm^{-1}$. Its PMR spectra showed NH peak at δ 10.09 (s, $1H_o$) has shown multiplate peak at δ 8.02-

7.96 (m, $1H_c$) and another peak at 7.41 (d, $J$ = 7.7 Hz, $1H_f$). Another aromatic protons of the compound were observed 7.38 (t, $J$ = 3.0 Hz, $1H_i$), 7.36 – 7.33 (m, $2H_{d,e}$), 7.32 – 7.29 (m, $2H_{b,h}$), 7.28 (dd, $J$ = 4.9, 3.2 Hz, $2H_{a,g}$), 7.25 – 7.21 (m, $2H_{k,l}$) and 7.20 – 7.15 (m, $1H_{,m}$). The aliphatic protons of the spacer were observed as a singlet at 5.44 (s, $2H_n$) and another singlet was observed at 2.45 (s, $3H_k$) for methyl protons. The mass spectrum of compound (**207**) showed molecular ion peak at m/z 523.0 $(M+2)^+$.

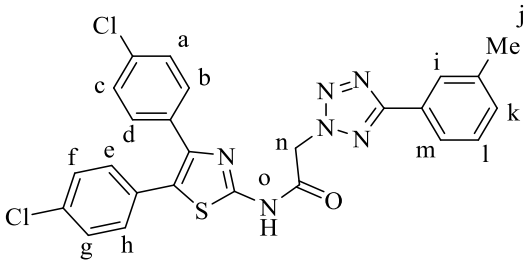


**(207)**

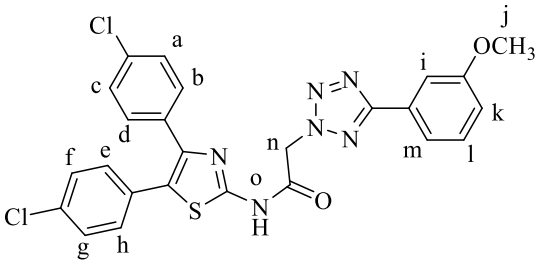


**(208)**

IR spectrum of synthesized compound (**208)** showed carbonyl stretching at 1697 $cm^{-1}$ along with the C-O peak at 1254 $cm^{-1}$. Its PMR spectra has showed multiplate peak at δ 8.11 (d, $J$ = 8.8 Hz, $2H_{c,f}$) and another peak at 7.50 (d, $J$ = 8.5 Hz, $1H_i$). Another aromatic proton of the compound were observed 7.39 – 7.34 (m, $2H_{d,e}$), 7.31 (d, $J$ = 4.3 Hz, $1H_k$), 7.28 (d, $J$ = 4.3 Hz, $2H_{l,m}$), 7.24 – 7.21 (m, $2H_{b,h}$) and 7.02 (d, $J$ = 8.8 Hz, $2H_{a,g}$). The aliphatic protons of the spacer were observed as a singlet at 5.40 (s, $2H_n$) and another singlet was observed at 3.88 (s, $3H_j$) for methoxy protons. The mass spectrum of compound (**208**) showed molecular ion peak at m/z 539.4 $(M+2)^+$.

IR spectrum of synthesized compound (**209)** showed NH stretching at 3334 $cm^{-1}$ and carbonyl stretching at 1690 $cm^{-1}$. Its PMR spectra showed NH peak at δ 10.62 (s, $1H_o$), the spectra has shown doublet over doublet peak at δ 8.00 (dd, $J$ = 7.6, 1.5 Hz, $1H_c$) and another peak at 7.93 (dd, $J$ = 8.0, 1.2 Hz, $1H_f$). Another aromatic protons of the compound were observed 7.74 (td, $J$ = 7.6, 1.4 Hz, $1H_i$), 7.68 (td, $J$ = 7.8, 1.5 Hz, $1H_m$), 7.42 – 7.37 (m, $2H_{k,l}$), 7.33 – 7.28 (m, $4H_{b,d,e,h}$), and 7.25 – 7.21 (m, $2H_{a,h}$). The aliphatic protons of the spacer were observed as a singlet at 5.28 (s, $2H_n$). The mass spectrum of compound (**209**) showed molecular ion peak at m/z 554.3 $(M+2)^+$.

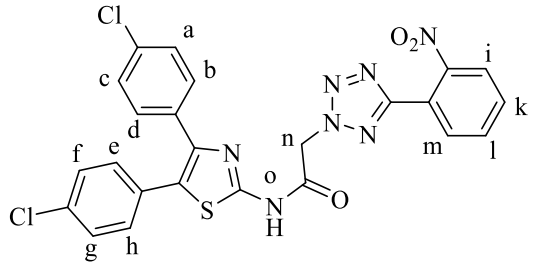

**(209)**

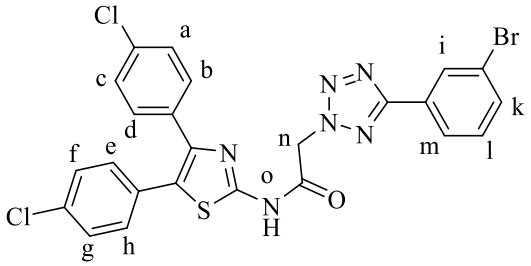

**(210)**

IR spectrum of synthesized compound (**210)** showed NH stretching at 3315 $cm^{-1}$ and carbonyl stretching at 1699 $cm^{-1}$. Its PMR spectra showed NH peak at δ 9.87 (s, $1H_o$), the spectra has shown triplet peak at δ 8.35 (t, *J* = 1.7 Hz, $1H_c$) and another peak at 8.12 (d, *J* = 7.8 Hz, $1H_f$). Another aromatic proton of the compound were observed at 7.65 (d, *J* = 8.1, $1H_i$), 7.41 (d, *J* = 7.9 Hz, $1H_k$), 7.37 (d, *J* = 8.6 Hz, $2H_{l,m}$), 7.34 – 7.27 (m, $4H_{b,d,e,h}$), and 7.25 – 7.21 (m, $2H_{a,h}$).The aliphatic protons of the spacer were observed as a singlet at 5.47 (s, $2H_n$).

IR spectrum of synthesized compound (**211)** showed NH stretching at 3225 $cm^{-1}$ and carbonyl stretching at 1702 $cm^{-1}$ along with the C-O peak at 1281 $cm^{-1}$. Its PMR spectra showed NH peak at δ 10.67 (s, $1H_o$), the spectra has shown doublet peak at δ 8.07 (d, *J* = 8.3 Hz, $2H_{c,f}$) and another peak at 7.39 – 7.33 (m, $4H_{i,j,l,m}$). Another aromatic protons of the compound were observed 7.33 – 7.29 (m, $2H_{d,e}$), 7.28 – 7.25 (m, $2H_{b,h}$), and 7.24 – 7.19 (m, $2H_{a,g}$). The aliphatic protons of the spacer were observed as a singlet at 5.26 (s, $2H_n$) along with doublet over doublet at 2.97 (dd, *J* = 13.8, 6.8 Hz, $1H_k$) and a multiplate for methyl groups at 2.95 (dd, *J* = 13.8, 6.8 Hz, $6H_{p,q}$). The mass spectrum of compound (**211**) showed molecular ion peak at m/z 551.3 $(M+2)^+$.

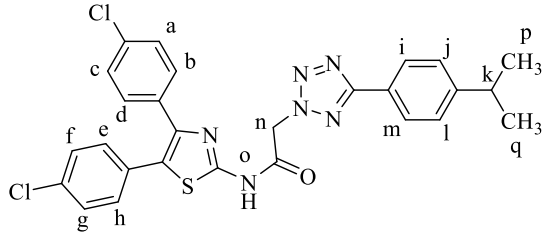

**(211)**

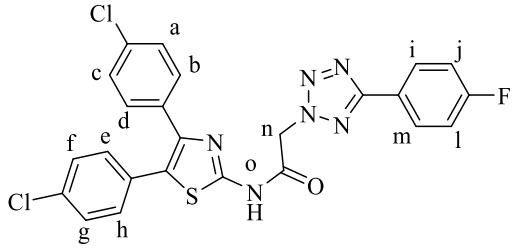

**(212)**

IR spectrum of synthesized compound (**212)** showed NH stretching at 3179

$cm^{-1}$ and carbonyl stretching at 1724 $cm^{-1}$ along with the C-O peak at 1268 $cm^{-1}$. Its PMR spectra has shown doublet over doublet peak at δ 8.17 (dd, *J* = 8.1, 5.1 Hz, $2H_{c,f}$) and another peak at 7.38 (dt, *J* = 8.9, 6.5, $2H_{j,l,}$). Another aromatic protons of the compound were observed 7.35 – 7.27 (m, $2H_{d,e,I,m}$), 7.23 (dd, *J* = 6.7, 1.9 Hz, $2H_{b,h}$), and 7.18 (ddd, *J* = 13.3, 6.8, 4.5 Hz,, $2H_{a,g}$). The aliphatic protons of the spacer were observed as a singlet at 5.35 (s, $2H_n$). The mass spectrum of compound (**212**) showed molecular ion peak at m/z 526.0 $(M+2)^+$.

IR spectrum of synthesized compound (**213)** showed carbonyl stretching at 1700 $cm^{-1}$ along with the carbonyl peak at 1254 $cm^{-1}$. Its PMR spectra showed a multiplate peak at 7.76-7.72 (m, $1H_c$) and a doublet at 7.66 (d, *J* = 2.8 Hz, $1H_f$). Another aromatic protons of the compound were observed at 7.53 (t, *J* = 2.8 Hz, $1H_i$), 7.43 – 7.39 (m, $2H_{a,g}$), 7.21 (dd, *J* = 8.6, 2.2 Hz, $1H_l$), 6.97 (d, *J* = 8.4 Hz, $1H_m$), 6.84 (dt, d, *J* = 8.4 Hz, $4H_{b,d,e,h}$). The aliphatic protons of the spacer were observed as a singlet at 4.96 (s, $2H_n$) and the six methoxy protons of vicinal diaryls were observed as a doublet at 3.98 (d, *J* = 4.6 Hz, $3H_p$), 3.95 (d, J = 3.3 Hz, $3H_q$), similarly protons of methoxy group attached to benzyl group of tetrazole were observed at 3.90 (d, J = 2.7 Hz, $3H_j$), 3.78 (d, J = 5.8 Hz, $3H_k$).

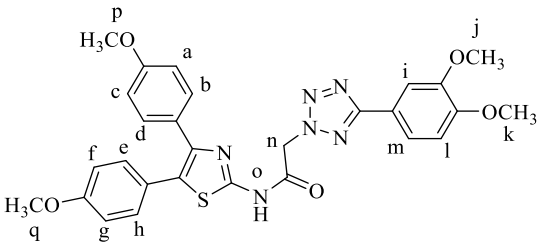


**(213)**

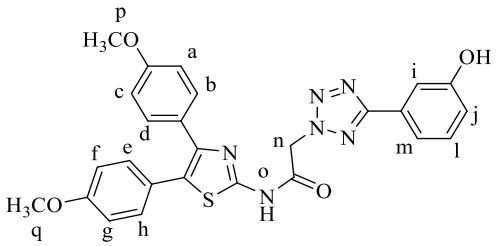


**(214)**

IR spectrum of synthesized compound (**214)** showed carbonyl stretching at 1698 $cm^{-1}$ along with the carbonyl peak at 1285 $cm^{-1}$. Its PMR spectra showed a doublet peak at δ 7.65 (d, *J* = 7.7 Hz, $1H_c$) and a multiplate at 7.56 – 7.52 (m, $1H_f$). Another aromatic protons of the compound were observed at 7.51 (t, *J* = 3.4 Hz, $1H_i$), 7.46 (d, *J* = 2.2 Hz, $1H_j$), 7.44 – 7.40 (m, $3H_{a,g,l}$), 7.32 (t, *J* = 8.0 Hz, $1H_m$), 7.23 – 7.18 (m, $1H_d$), 6.93 (dd, *J* = 8.1, 1.9 Hz, $1H_e$), 6.87 (d, *J* = 4.9 Hz, $1H_b$), 6.77 (d, *J* = 8.8 Hz, $1H_h$). The aliphatic protons of the spacer were observed as a singlet at 4.84 (s, $2H_n$) and the six methoxy protons of vicinal diaryls were observed as a multiplate at 3.92-3.89 (m, $3H_p$), 3.80 (d, J = 3.3 Hz, $3H_q$). The mass spectrum of compound (**214**) showed molecular ion

peak at m/z at 515.3 $(M+1)^+$.

IR spectrum of synthesized compound (**215)** showed carbonyl stretching at 1699 $cm^{-1}$ along with the carbonyl peak at 1282 $cm^{-1}$. Its PMR spectra has shown multiplate peak at 8.10-8.04 (m, $2H_{c,\ f}$) and another peak at 7.52 (t, $J$ = 2.8 Hz, $1H_a$). Another aromatic protons of the compound were observed at 7.21 (dt, $J$ = 12.9, 3.2 Hz, $1H_g$), 7.03 – 6.97 (m, $3H_{d,j,l}$), 6.89 – 6.85 (m, $3H_{e,I,m}$) and 6.84 – 6.79 (m, $2H_{b,h}$). The aliphatic protons of the spacer were observed as a singlet at 4.86 (s, $2H_n$) and the six methoxy protons of vicinal diaryls were observed as a multiplate at 3.92-3.88 (m, $3H_p$), 3.87 (m, $3H_q$) and the methoxy proton on tetrazole substitute benzene were observed as a doublet at 3.78 (d, J = 3.8 Hz, $3H_k$). The mass spectrum of compound (**215**) showed molecular ion peak at m/z at 528.2 $(M)^+$.

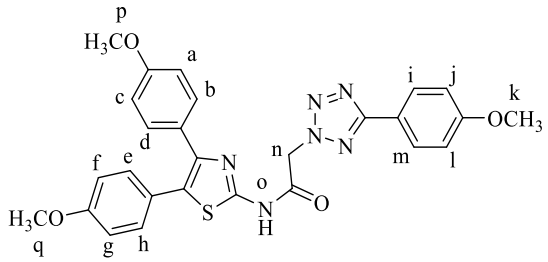


**(215)**

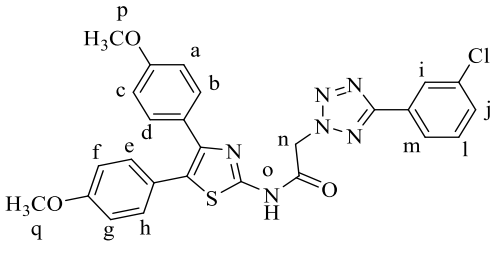


**(216)**

IR spectrum of synthesized compound (**216)** showed carbonyl stretching at 1700 $cm^{-1}$ along with the carbonyl peak at 1283 $cm^{-1}$. Its PMR spectra showed a multiplate peak at δ 8.13 (d, $J$ = 1.7 Hz $1H_c$) and a doublet over triplet at 8.02 (dt, $J$ = 7.0, 1.6 Hz, $1H_f$). Another aromatic protons of the compound were observed at 7.51 (d, $J$ = 2.2 Hz, $1H_i$), 7.47 – 7.40 (m, $4H_{a,g,j,l,}$), 7.24 – 7.19 (m, $1H_m$), 6.88 (dd, $J$ = 8.5, 5.5 Hz, $2H_{d,e}$) and 6.83 (dt, $J$ = 7.5, 4.3 Hz, $2H_{b,h}$). The aliphatic protons of the spacer were observed as a singlet at 4.66 (s, $2H_n$) and the six methoxy protons of vicinal diaryls were observed as a doublet at 3.91-3.88 (m, $3H_p$), 3.79 (d, J = 3.4 Hz, $3H_q$). The mass spectrum of compound (**216**) showed molecular ion peak at m/z 533.1 $(M)^+$.

IR spectrum of synthesized compound (**217)** showed carbonyl stretching at 1706 $cm^{-1}$ along with the carbonyl peak at 1278 $cm^{-1}$. Its PMR spectra showed a multiplate peak at δ 8.03 – 7.98 (m, $2H_{c,f}$) and a multiplate at 7.65 – 7.61 (m, $2H_{j,l}$). Another aromatic protons of the compound were observed at 7.52 (t, $J$ = 2.9 Hz, $1H_b$), 7.46 – 7.40 (m, $2H_{i,m}$), 7.23 – 7.19 (m, $1H_h$), 6.90 – 6.86 (m, $2H_{d,e}$), 6.82 (dd, $J$ = 11.4,

6.0 Hz, $2H_{a,g}$). The aliphatic protons of the spacer were observed as a singlet at 4.78 (d, $J$ = 19.1 Hz, $2H_n$) and the six methoxy protons of vicinal diaryls were observed as a multiplate at 3.91 – 3.88 (m, $3H_p$), 3.78 (d, $J$ = 3.9 Hz, $3H_q$). It's $^{13}C$ spectra showed carbonyl peak at 164.76 and aromatic carbon peaks at 162.41, 160.10, 157.25, 155.77, 143.43, 133.85, 132.11, 130.48, 130.28, 129.50, 128.43, 126.10, 125.85, 125.20, 124.95, 124.64, 114.66, 114.35, 111.99. The aliphatic carbon peaks were observed at 56.25, 55.34, 53.36. The mass spectrum of compound (**217**) showed molecular ion peak at m/z at 577.1 $(M)^+$.

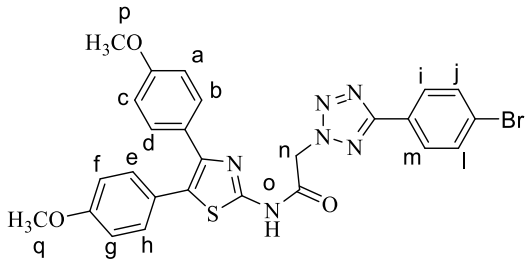


**(217)**

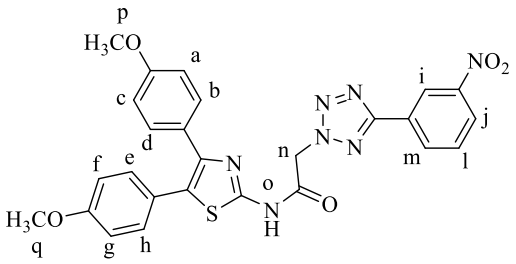


**(218)**

IR spectrum of synthesized compound (**218)** showed carbonyl stretching at 1699 $cm^{-1}$ along with the carbonyl peak at 1248 $cm^{-1}$. Its PMR spectra showed a doublet peak at δ 9.00 (d, $J$ = 1.7 Hz, $1H_c$) and a multiplate at 8.50 (d, $J$ = 7.8 Hz, $1H_f$). Another aromatic protons of the compound were observed at 8.38 – 8.32 (m, $1H_i$), 7.71 (t, $J$ = 8.0 Hz, $2H_{j,l}$), 7.51 (dd, $J$ = 10.0, 4.4 Hz, $1H_m$), 7.46 – 7.40 (m, $2H_{d,e}$), 6.92 – 6.86 (m, $2H_{a,g}$) and 6.84 – 6.80 (m, $2H_{b,h}$). The aliphatic protons of the spacer were observed as a singlet at 4.88 (d, $J$ = 18.8 Hz, $2H_n$) and the six methoxy protons of vicinal diaryls were observed as a multiplate at 3.91 – 3.88 (m, $3H_p$), 3.80 (d, $J$ = 3.1 Hz, $3H_q$). The mass spectrum of compound (**218**) showed molecular ion peak at m/z at 543.2 $(M)^+$.

IR spectrum of synthesized compound (**219)** showed carbonyl stretching at 1701 $cm^{-1}$ along with the carbonyl peak at 1283 $cm^{-1}$. Its PMR spectra showed a multiplate peak at δ 8.03 (d, $J$ = 8.2 Hz, $2H_{c,f}$) and a doublet peak at 7.52 (d, $J$ = 2.2 Hz, $1H_b$). Another aromatic protons of the compound were observed at 7.40 (d, $J$ = 8.8 Hz, $2H_{d,e}$), 7.30 (d, $J$ = 8.0 Hz, $2H_{a,g}$7.21 (dd, $J$ = 8.5, 2.2 Hz, $1H_h$), 6.86 (d, $J$ = 8.8 Hz, $2H_{j,l}$) and 6.81 (dd, $J$ = 15.1, 5.9 Hz, $2H_{i,m}$). The aliphatic protons of the spacer were observed as a singlet at 5.03 (d, $J$ = 20.3 Hz, $2H_n$) and the six methoxy protons of vicinal diaryls were observed as a doublet at 3.91 (d, $J$ = 5.4 Hz, $3H_p$), and singlet 3.79 (s, $3H_q$) also the protons of methyl group was observed at 2.42 (s, $3H_k$). Its $^{13}C$ NMR showed

carbonyl peak at 165.68 and aromatic carbon peaks were observed at 162.50, 160.03, 157.09, 155.70, 143.49, 140.71, 133.87, 130.26, 129.52, 126.85, 126.14, 125.08, 124.77, 124.05, 114.59 and 111.93. The aliphatic carbon peak was observed at 56.23, 55.33, 53.40 and 21.50. The mass spectrum of compound (**219**) showed molecular ion peak at m/z at 511.3 $(M-1)^-$.

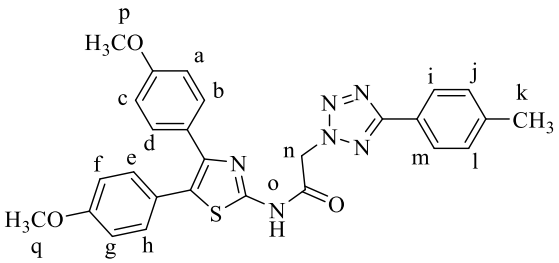

**(219)**

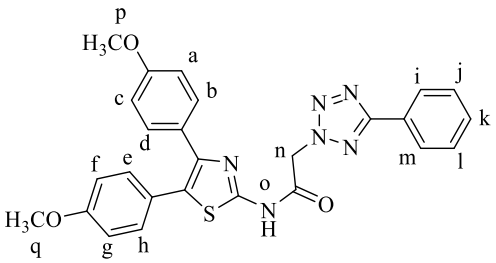

**(220)**

IR spectrum of synthesized compound (**220)** showed carbonyl stretching at 1702 $cm^{-1}$ along with the carbonyl peak at 1283 $cm^{-1}$. Its PMR spectra showed a multiplate peak at δ 8.18 – 8.09 (m, $2H_{c,f}$) and a doublet peak at 7.50 (dd, $J$ = 6.7, 5.2, 3.2 Hz, $4H_{b,d,e,h}$). Another aromatic protons of the compound were observed at 7.43 – 7.40 (m, $2H_{a,g}$), 7.21 (dd, $J$ = 8.5, 2.2 Hz, $1H_k$ ), 6.90 – 6.86 (m, $2H_{i,m}$), and 6.80 (dd, $J$ = 18.3, 8.6 Hz, $2H_{j,l}$). The aliphatic protons of the spacer were observed as a singlet at 4.90 (s, $2H_n$) and the six methoxy protons of vicinal diaryls were observed as a multiplate at 3.92 – 3.87 (m, $3H_p$), and singlet 3.79 (s, $3H_q$).

IR spectrum of synthesized compound (**221)** showed carbonyl stretching at 1700 $cm^{-1}$ along with the C-O peak at 1283 $cm^{-1}$. Its PMR spectra showed a multiplate peak at δ 7.98 – 7.91 (m, $2H_{c,f}$) and a triplet peak at 7.52 (t, $J$ = 2.7 Hz, $1H_b$). Another aromatic protons of the compound were observed at 7.44 – 7.38 (m, $2H_{d,e}$), 7.37 (d, $J$ = 7.6 Hz, $1H_i$ ), 7.32 – 7.26 (m, $1H_k$), 7.21 (dd, $J$ = 8.5, 2.2 Hz, $1H_h$), 6.90 – 6.85 (m, $2H_{l,m}$) and 6.85 – 6.73 (m, $2H_{a,g}$). The aliphatic protons of the spacer were observed as a singlet at 4.88 (d, $J$ = 20.7 Hz, $2H_n$) and the six methoxy protons of vicinal diaryls were observed as a doublet at 3.92-3.87 (m, $3H_p$), and a multiplate 3.82-3.77 (m, $3H_q$) also the protons of methyl group were observed at 2.44 (d, $J$ = 5.2 Hz, $3H_k$). The mass spectrum of compound (**221**) showed molecular ion peak at m/z at 513.4 $(M+1)^+$ .

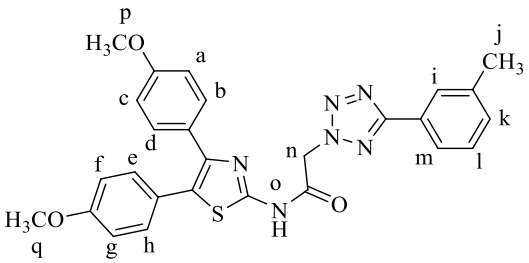

**(221)**

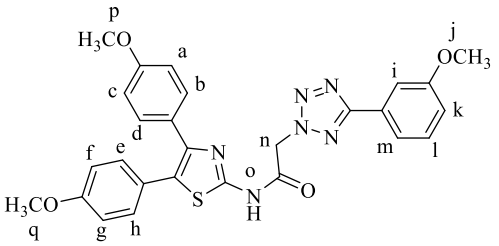

**(222)**

IR spectrum of synthesized compound (**222)** showed carbonyl stretching at 1724 $cm^{-1}$ along with the carbonyl peak at 1277 $cm^{-1}$. Its PMR spectra has shown multiplate peak at δ 8.21 (d, *J* = 1.8 Hz, $1H_c$) and another peak at 7.93 – 7.90 (m, $1H_f$). Another aromatic protons of the compound were observed at 7.75 – 7.69 (m, $2H_{d,e}$), 7.52 (d, *J* = 2.2 Hz, $1H_i$), 7.42 – 7.40 (m, $2H_{b,h}$), 7.22 – 7.20 (m, $1H_k$), 6.96 (d, *J* = 4.4 Hz, $1H_m$), 6.86 (d, *J* = 1.2 Hz, $1H_l$) and 6.85 – 6.80 (m, $2H_{a,g}$). The aliphatic protons of the spacer were observed as a singlet at 5.01 (s, $2H_n$) and the six methoxy protons of vicinal diaryls were observed as a multiplate at 3.99 (m, $3H_p$), 3.90 (d, *J* = 2.5 Hz, $3H_q$) and the methoxy proton peak on tetrazole substituted benzene were observed as a singlet at 3.79 (s, $3H_j$). The mass spectrum of compound (**222**) showed molecular ion peak at m/z at 528.2 $(M)^+$.

IR spectrum of synthesized compound (**223)** showed carbonyl stretching at 1798 $cm^{-1}$ along with the carbonyl peak at 1284 $cm^{-1}$. Its PMR spectra showed a doublet peak at δ 7.96 (dt, *J* = 6.4, 3.2 Hz, $1H_c$) and a doublet over doublet at 7.90 (dd, *J* = 8.0, 1.4 Hz,$1H_f$). Another aromatic protons of the compound were observed at 7.76 – 7.69 (m, $1H_j$), 7.69 – 7.62 (m, $1H_m$7.51 (dq, *J* = 6.6, 3.2 Hz, $1H_k$), 7.44 (dd, *J* = 8.8, 2.0 Hz, $2H_{d,e}$), 7.22 (dd, *J* = 9.1, 2.7 Hz, $1H_l$), 6.92 – 6.86 (m, $2H_{b,h}$) and 6.85 – 6.80 (m, $2H_{a,g}$). The aliphatic protons of the spacer were observed as a singlet at 4.79 (d, *J* = 13.7 Hz, $2H_n$) and the six methoxy protons of vicinal diaryls were observed as a multiplate at 3.92 – 3.88 (m, $3H_p$), 3.80 (t, *J* = 4.9 Hz, $3H_q$). The mass spectrum of compound (**223**) showed molecular ion peak at m/z at 543.3 $(M)^+$.

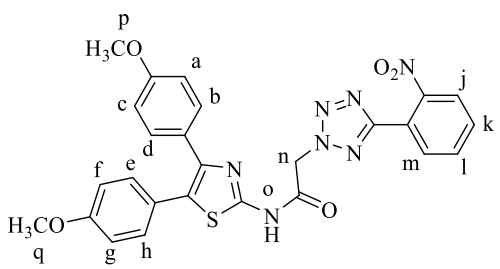

**(223)**

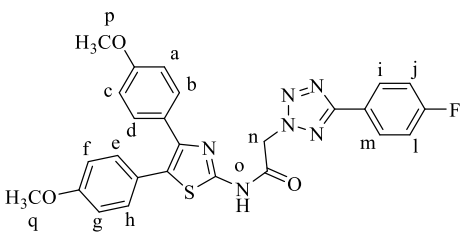

**(224)**

IR spectrum of synthesized compound (**224)** showed carbonyl stretching at 1731 $cm^{-1}$ along with the carbonyl peak at 1305 $cm^{-1}$. Its PMR spectra showed a multiplate peak at δ 8.16-8.10 (m, $2H_{c,f}$) and a doublet peak at 7.52 (d, *J* = 2.2 Hz, $1H_b$). Another aromatic protons of the compound were observed at 7.45 – 7.38 (m, $2H_{j,l}$), 7.20 (t, *J* = 4.2 Hz, $1H_h$ ), 7.19 – 7.13 (m, $2H_{i,m}$), 6.91-6.86 (m, $2H_{d,e}$) and 6.84 (dd, *J* = 8.9, 5.8 Hz, $2H_{a,g}$). The aliphatic protons of the spacer were observed as a singlet at 4.81 (d, *J* = 19.2 Hz, $2H_n$) and the six methoxy protons of vicinal diaryls were observed as a doublet at 3.92-3.88 (m, $3H_p$), and a multiplate 3.80-3.76 (m, $3H_q$). Its $^{13}C$ NMR showed carbonyl peak at 165.36 and aromatic carbon peaks observed at 164.78, 162.87, 162.46, 160.09, 159.93, 159.50, 157.20, 155.76, 143.45, 142.67, 133.86, 130.49, 130.27, 129.51, 129.03, 128.95, 126.11, 125.17, 124.67, 123.16, 116.11, 115.89, 114.64, 114.34, 111.98. The aliphatic carbon peaks were observed at 56.25, 55.32, 53.36. The mass spectrum of compound (**224**) showed molecular ion peak at m/z at 516.2 $(M)^+$.

### 4.1.2 Synthesis of 2-(2-substititedethyl)isoindoline-1,3-dione for general scheme 2

Phthalimide based compounds (**263-275, 288-297**) were synthesized using various strategies as discussed in **general scheme 2**.

2-(2-Bromoethyl)isoindoline-1,3-dione was heated with liquid ammonia at 40$^oC$ under solvent free conditions to offer 2-(2-aminoethyl)isoindoline-1,3-dione. The resulted compound was further condensed with different substituted chalcones in the presence of base and anhy. DMF to offer desired compounds (**263-275).**

1-(2-(1,3-Dioxoisoindolin-2-yl)ethyl)piperidine-4-carboxamide was synthesized on condensation of 2-(2-bromoethyl)isoindoline-1,3-dione with isonipecotamide which was further reacted with substituted benzyl halides to yield final desired compounds **(288-297**).

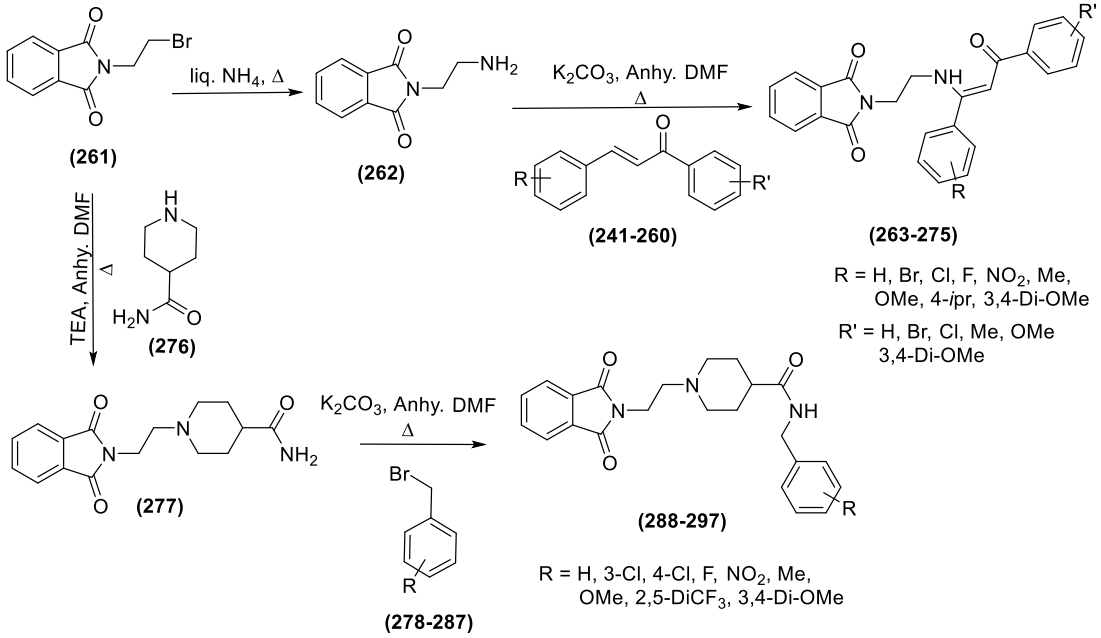


**General scheme 2**: Synthesis of 2-(2-substititedethyl)isoindoline-1,3-dione **(263-275)** and **(288-297)**

For the synthesis of desired compounds benzaldehyde, acetophenone, liq. ammonia, sodium hydroxide, isonipecotamide and dimethylformamide were procured directly from the market. The steps followed for the synthesis of compounds (**263-275**) are discussed under following headlines.

**4.1.2.1** Synthesis of substituted chalcones (**241-260**)

**4.1.2.2** Synthesis of 2-(2-aminoethyl)isoindoline-1,3-dione (**262**)

**4.1.2.3** Synthesis of (*Z*)-2-(2-((3-oxo-1,3-diphenylprop-1-en-1-yl)amino)ethyl)isoindol -ine-1,3-dione derivatives (**263-275**)

**4.1.2.1 Synthesis of substituted chalcones (241-260)**

Different chalcones were synthesized by following Claisen Schmidt condensation reaction in which substituted benzaldehydes were reacted with substituted acetophenone in the presence of sodium hydroxide as base and water as solvent in ice-cold conditions. The synthesized chalcones were characterized using IR spectra which showed carbonyl peak between 1625-1720 $cm^{-1}$.

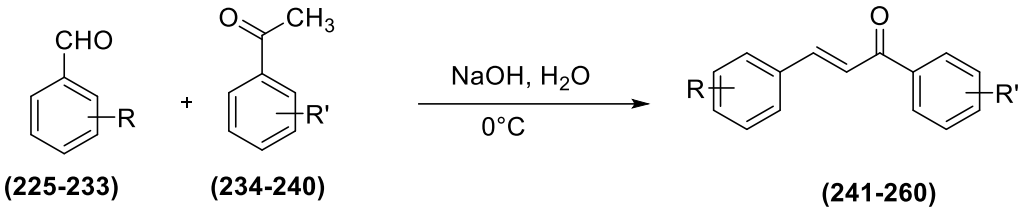


**(225-233)** **(234-240)** **(241-260)**

R = H, Br, Cl, F, $NO_2$, Me, OMe,

**Scheme 9**

### 4.1.2.2 Synthesis of 2-(2-aminoethyl)isoindoline-1,3-dione (262)

Isoindoline derivative has been synthesized by condensation of liquid ammonia with 2-(2-bromoethyl)-1*H*-indene-1,3(2*H*)-dione in oil bath at 50ºC for 1-2hr. The synthesized compound were characterized using IR spectra with peaks at 3124, 2874 and 1731$cm^{-1}$.

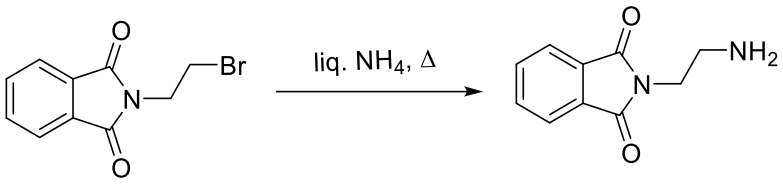


**(261)** **(262)**

**Scheme 10**

### 4.1.2.3 Synthesis of (*Z*)-2-(2-((3-oxo-1,3-diphenylprop-1-en-1-yl)amino)ethyl) isoindoline-1,3-dione derivatives (263-275)

2-(2-Aminoethyl)isoindoline-1,3-dione on condensation with different chalcone derivatives in the presence of base potassium carbonate and solvent anhy. DMF resulted in the synthesis of (*Z*)-2-(2-((3-oxo-1,3-diphenylprop-1-en-1-yl)amino)ethyl)isoindoline-1,3-dione derivatives. The synthesized compounds were characterized using IR, mass and NMR.

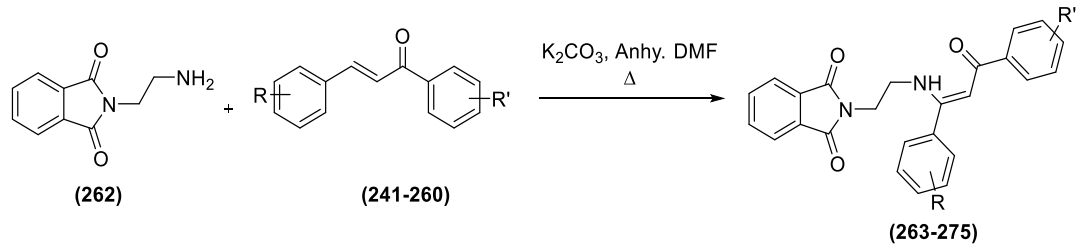


**(262)** **(241-260)** **(263-275)**

R = H, Br, Cl, F, $NO_2$, Me, OMe,
R' = H, Br, Cl, Me, OMe,

**Scheme 11**

IR spectrum of synthesized compound (**263)** showed secondary amine peak at 2987 $cm^{-1}$ and carbonyl peak at 1736 $cm^{-1}$. Its PMR spectra also showed a doublet peak at δ 8.02 (d, J = 9.0 Hz, $2H_{n,o}$), a doublet at 7.79 (d, J = 15.6 Hz, $1H_m$) along with a multiplate peak at 7.67 – 7.53 (m, $3H_{a,d,p}$) and doublet peak at 7.40 (d, J = 5.6 Hz, $2H_{b,c}$). The aromatic protons also showed a singlet peak at 7.26 (s, $3H_{h,i,j}$) and a doublet peak at 6.71 (d, J = 9.0 Hz, $2H_{k,g}$). Similarly, the aliphatic protons also showed a singlet at 3.09 (s, $2H_e$) for two protons along with a singlet at 1.56 (s, $2H_f$) and 1.25 (s, $1H_l$). The mass spectrum of compound (**263**) showed molecular ion peak at m/z at 415.27 $(M+1)^+$.

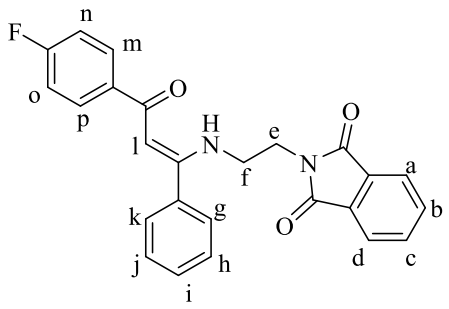


**(263)**

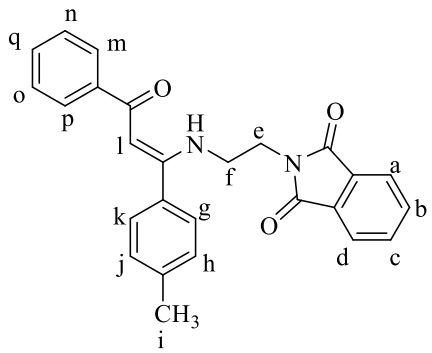


**(264)**

IR spectrum of synthesized compound **(264)** showed a secondary amine peak at 2955 $cm^{-1}$ and a carbonyl peak at 1730 $cm^{-1}$. Its PMR spectra showed a doublet for six protons at δ 8.00 (d, J = 6.9 Hz, $6H_{a,d,g,h,j,k}$), along with a doublet at 7.27 (d, J = 9.9 Hz, $7H_{b,c,m,n,o,p,q}$) for seven protons in aromatic region. Similarly, the aliphatic protons showed singlet peak at different positions i.e. at δ 3.50 (s, $1H_l$) for one proton, at δ 2.44 (s, $4H_{e,f}$) for four protons, at δ 1.25 (s, $1H_r$) for one proton and at δ 0.88 (s, $3H_i$) for three protons. The mass spectrum of compound (**264**) showed molecular ion peak at m/z at 409.00 $(M+1)^{+1}$.

IR spectrum of synthesized compound (**265)** showed a secondary amine peak at 2984 $cm^{-1}$ and carbonyl peak at 1736 $cm^{-1}$. Its PMR spectrum showed singlet peak of aromatic proton at δ 9.86 (s, 1H) for one proton, and a doublet peak at 8.02 (d, J = 7.3 Hz, $2H_{j,h}$). Other aromatic protons of this compound were observed as a singlet at 7.81 (s, $1H_a$) for one proton, as a singlet at 7.77 (s, $1H_d$) for one proton, as a doublet at 7.53 (d, J = 17.3 Hz, $3H_{m,n,p}$) for three protons along with different peaks at 7.42 (d, J = 15.6 Hz, $1H_{g,}$), 7.26 (s, $1H_k$), 6.99 (s, $2H_{b,c}$) and 6.90 (d, J = 8.6 Hz, $2H_{q,o}$). Similarly, the aliphatic protons showed singlet peak for five different protons at δ 3.52 (s, $1H_l$), 1.73

(s, $4H_{e,f}$) and 1.25 (s, $1H_r$). The mass spectrum of this compound (**265**) showed molecular ion peak at m/z 413.06 $(M+1)^+$.

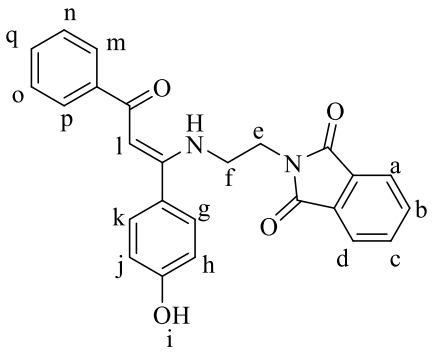

**(265)**

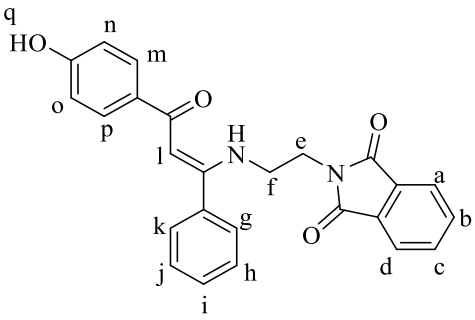

**(266)**

IR spectrum of synthesized compound (**266)** showed a secondary amine peak at 2956 $cm^{-1}$ and a carbonyl peak at 1734$cm^{-1}$. Its PMR spectrum showed a doublet over doublet peak at δ 7.98 (dd, J = 19.7, 8.7 Hz, $1H_n$) for one proton and a multiplate at 7.94 – 7.86 (m, $2H_{m,,o}$) for two protons. Similarly other protons of aromatic region were observed at 7.82 (d, J = 15.7 Hz, $1H_p$), 7.69 – 7.55 (m, $1H_a$), 7.55 – 7.46 (m, $1H_d$), 7.44 – 7.35 (m, $2H_{b,c}$), 7.26 (s, $1H_g$), 7.04 – 6.99 (m, $1H_k$), 6.98 – 6.92 (m, $2H_{h,j}$) and 6.90 (d, J = 8.7 Hz, $1H_i$). The aliphatic protons were observed as a singlet at δ 3.73 (s, $1H_l$) for one proton and a singlet at δ 2.57 (s, $4H_{e,f}$) for four protons. The mass spectrum of this compound (**266**) showed molecular ion peak at m/z 413.33 $(M+1)^+$.

IR spectrum of compound (**267)** showed secondary amine peak at 2983 $cm^{-1}$ and a carbonyl peak at 1737 $cm^{-1}$. Its PMR spectrum showed a multiplate at δ 8.15 – 7.56 (m, $6H_{a,d,g,k,n,o}$) for six aromatic protons along with a multiplate at 7.48 – 7.04 (m, $2H_{m,p}$), and a triplet at 6.66 (t, J = 11.4 Hz, $5H_{b,c,h,i,j}$) for five protons. Aliphatic protons of this compound has been observed as a singlet at 4.12 (s, $4H_{e,f}$) for four protons and a singlet at 1.62 (s, $1H_r$) for one proton in its PMR. The mass spectrum of compound (**267)** showed molecular ion peak at m/z 411.25 $(M)^+$.

IR spectrum of synthesized compound (**268)** showed secondary amine peak at 2983 $cm^{-1}$ and carbonyl peak at 1736 $cm^{-1}$. Its PMR spectrum showed a doublet at 7.93 (d, J = 8.9 Hz, $2H_{o,n}$) for two protons, a multiplate at 7.80 – 7.65 (m, $1H_h$) for one proton and a multiplate at 7.61 – 7.46 (m, $1H_j$). Another peak of aromatic protons has been observed at 7.42 (d, J = 8.0 Hz, $2H_{m,p}$), 7.25 – 7.10 (m, $3H_{a,d,g}$), 7.03 (d, J = 8.9 Hz,

$2H_{b,c}$), 6.88 – 6.74 (m, $1H_k$). The aliphatic protons shows a singlet peak at 5.94 (s, $1H_l$), along with a doublet over doublet peak at 2.99 (dd, J = 17.4, 10.7 Hz, $4H_{e,f}$) for four protons, other protons of aliphatic region were observed at 2.55 (s, $1H_r$), and 1.25 (s, $3H_i$). The mass spectrum of compound (**268**) showed a molecular ion peak at 426.43 ($M^+$).

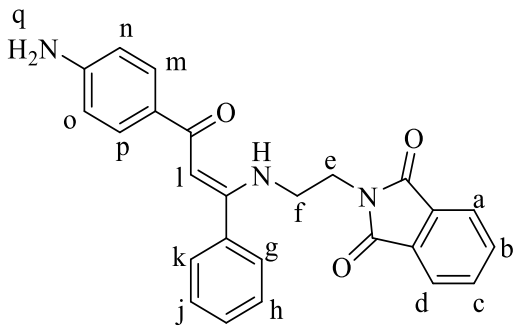


**(267)**

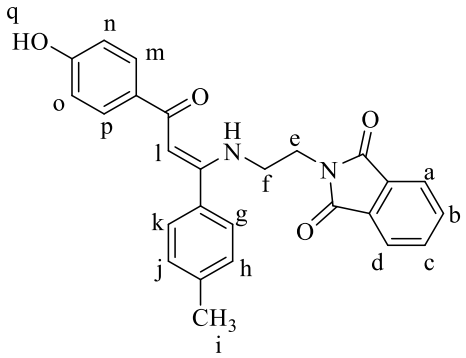


**(268)**

IR spectrum of synthesized compound (**269)** showed amine peak at 2984 $cm^{-1}$ and a carbonyl peak at 1736 $cm^{-1}$. Its PMR spectra showed a multiplate peak at δ 8.05 – 7.71 (m, $3H_{i,k,h}$) for three protons, a singlet was observed at 7.26 (s, $7H_{a,d,g,m,n,o,p}$) and a multiplate at 7.04 – 6.71 (m, $2H_{b,c}$) for three protons. The aliphatic proton peaks were observed as a singlet at 4.69(s, $1H_l$) and 2.56 (s, $4H_{e,f}$). The mass spectrum of compound (**269**) showed molecular ion peak at 493.01 $(M+2)^{+2}$.

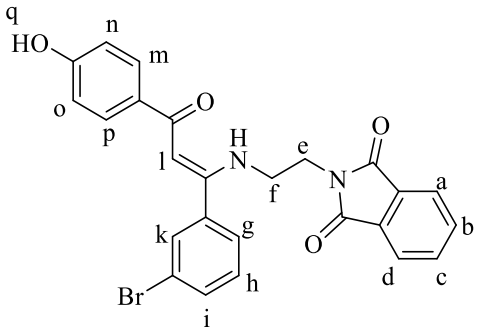


**(269)**

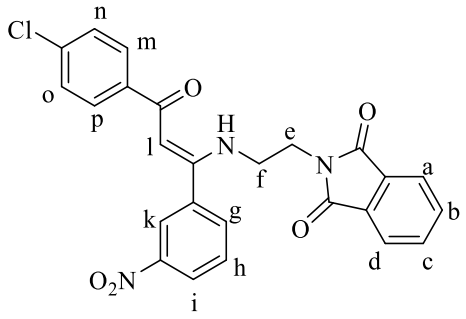


**(270)**

IR spectrum of synthesized compound (**270)** showed amine peak at 2922 $cm^{-1}$ and a carbonyl peak at 1736 $cm^{-1}$. Its PMR spectrum showed a triplet peak at δ 8.52 (t, J = 1.9 Hz, $1H_k$), a doublet over doublet peak at 8.28 (dd, J = 8.2, 2.1, 0.9 Hz, $1H_i$). Another peak of aromatic proton was observed at 8.06 – 7.98 (m, $2H_{n,o}$), 7.93 (d, J =

7.7 Hz, $1H_a$), 7.85 (d, J = 15.7 Hz, $1H_d$), 7.62 (d, J = 15.6 Hz, $2H_{m,p}$), 7.52 (d, J = 8.6 Hz, $2H_{b,c}$), 7.46 – 7.32 (m, $1H_g$) and 7.00 (s, $1H_h$) for different protons. The aliphatic protons showed a doublet peak at 3.49 (d, J = 5.3 Hz, $1H_l$) and other singlet peaks at 1.56 (s, $3H_i$), 1.25 (s, $2H_{e,}$) and 0.88 (s, $2H_f$). The mass spectrum of compound (**270**) showed a molecular ion peak at 475.86 (M+1).

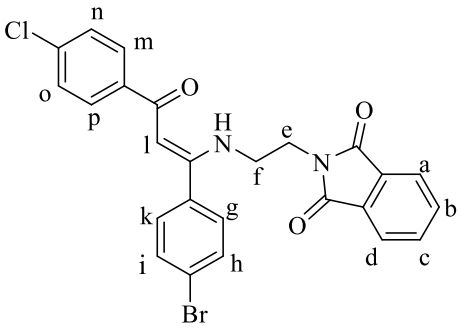


**(271)**

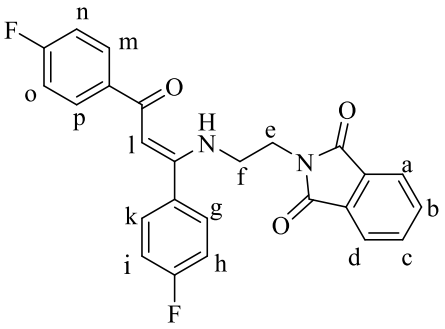


**(272)**

IR spectrum of synthesized compound (**271)** showed amine peak at 2985 $cm^{-1}$ and a carbonyl peak at at 1735 $cm^{-1}$. Its PMR spectrum showed a multiplate peak at δ 7.90 – 7.82 (m, $3H_{h,n,i}$) for three protons, a doublet at 7.52 (d, J = 4.5 Hz, $1H_o$) for one proton, a multiplate at 7.45-7.37 (m, $5H_{m,p.a,d,g}$) for five protons. Other aromatic protons show a doublet over doublet peak at 7.14 (dd, J = 11.4, 4.9 Hz, $2H_{b,c,}$) for three protons and a doublet at 6.98 (d, J = 11.3 Hz, $1H_k$) for one proton. The aliphatic protons show a triplet peak at 2.17 (t, J = 5.5 Hz, $1H_l$) for one proton and a singlet at 1.25 (s, $4H_{e,f}$) for four protons. The mass spectrum of compound (**271**) showed molecular ion peak at 510.94 $(M+1)^+$.

IR spectrum of synthesized compound **(272)** showed amine peak at 2983 $cm^{-1}$ and a carbonyl peak at 1736 $cm^{-1}$. Its PMR spectra showed a multiplate peak at δ 8.01 – 7.99 (m, $2H_{h,i}$) for two protons, a doublet at 7.75 (d, J = 15.6 Hz, $1H_a$) for one proton, a multiplate at 7.65 – 7.61 (m, $2H_{n,o}$) for two protons and a doublet at 7.53 (d, J = 5.4 Hz, $1H_d$). Other aromatic proton peaks were observed as a singlet at 7.49 (s, $1H_m$) for one proton, a multiplate at 7.11 – 7.07 (m, $2H_{g,k}$) for two protons, and at 6.73 – 6.67 (m, $3H_{b,c,p}$) for three protons. Aliphatic proton peaks were observed as a doublet at 3.06 (d, J = 2.7 Hz, $1H_q$) for one proton, as a singlet at 1.59 (s, $2H_f$) for two protons and as a doublet over doublet at 1.28 (dd, J = 26.6, 14.1 Hz, $2H_e$) for two protons. The mass spectrum of compound (**272**) showed molecular ion peak at 432.57 $(M^+)$.

IR spectrum of synthesized compound (**273)** showed amine group peak at 2956 $cm^{-1}$ and carbonyl peak at 1732 $cm^{-1}$. Its PMR spectra showed aromatic proton peak as a multiplate at 8.02 – 7.99 (m, $3H_{h,i,n}$) for three protons, as a doublet at 7.77 (d, J = 15.6 Hz, $2H_{a,b}$) for two protons, and at 7.54 (d, J = 7.1 Hz, $3H_{o,m,p}$) for three protons. Other aromatic proton peaks were observed as a singlet at 7.20 (s, $2H_{g,k}$) for two protons and as a multiplate at 6.71 – 6.69 (m, $2H_{b,c}$) for two protons. The aliphatic protons showed a singlet peak at 5.30 (s, $1H_l$) for one proton, a doublet at 3.06 (d, J = 2.2 Hz, 1H) for one proton, and as a multiplate at 2.39 (s, $3H_q$) for three protons and a doublet at 1.28 (d, J = 5.3 Hz, 4H) for four protons. The mass spectrum of compound (**273**) showed molecular ion peak at 427.3 $(M-1)^-$.

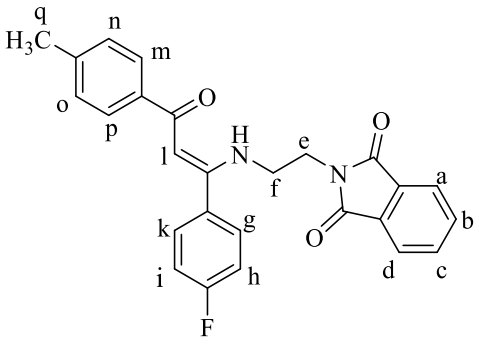


**(273)**

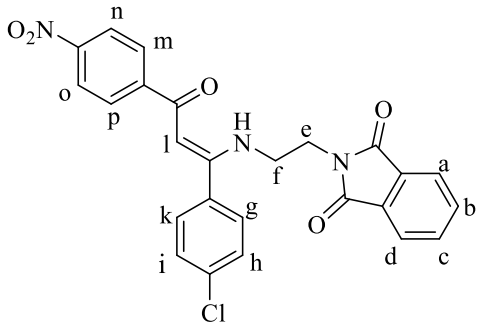


**(274)**

IR spectrum of synthesized compound (**274**) showed amine group peak 2984 $cm^{-1}$ and carbonyl group peak at 1736 $cm^{-1}$. Its PMR spectra showed a multiplate peak at δ 8.43 – 8.22 (m, $2H_{h,i}$) for two protons, a multiplate at 8.23 – 7.99 (m, $2H_{n,o}$). The aromatic proton showed a doublet over doublet peak at 7.90 (dd, J = 28.5, 8.8 Hz, $2H_{a,d}$) for two protons and at 7.67 (dd, J = 19.1, 7.6 Hz, $1H_m$) for one proton. Other aromatic protons were also observed as a doublet over doublet at 7.53 (dd, J = 15.8, 7.7 Hz, $1H_p$) for one proton, as a multiplate at 7.40 – 7.31 (m, $2H_{g,k}$) for two protons, as a doublet at 6.99 (d, J = 7.7 Hz, $1H_b$) for one proton and a doublet over doublet at 6.68 (dd, J = 22.7, 8.4 Hz, $1H_c$) for one proton. The aliphatic proton peaks were observed as a multiplate at 5.39 – 5.22 (m, $1H_q$) for one proton, as a singlet at 2.51 (s, $1H_l$), and as a triplet at 1.29 (t, J = 14.8 Hz, $4H_{e,f}$) for four protons. The mass spectrum of compound (**274**) showed molecular ion peak at 474.96 $(M+1)^+$.

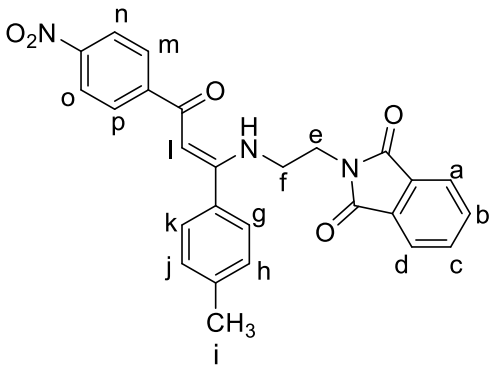

**(275)**

IR spectrum of synthesized compound (**275)** showed amine group peak at 2956 $cm^{-1}$ and carbonyl group peak at 1599 $cm^{-1}$. Its PMR spectra showed a doublet over doublet peak at 8.06 (dd, J = 11.1, 5.2 Hz, $1H_n$) for one proton, as a doublet over doublet peak at 7.99 (dd, J = 19.8, 10.1 Hz, $1H_o$) for one proton, as a multiplate at 7.95 – 7.89 (m, $1H_h$), 7.89 – 7.80 (m, $2H_{a,d}$). Other aromatic proton peaks were observed as a multiplate at 7.61 – 7.48 (m, $3H_{j,m,p}$) for three protons, 7.02 – 6.98 (m, $1H_g$), 6.77 – 6.64 (m, $2H_{b,c}$) and as a doublet at 6.60 (d, J = 7.7 Hz, $1H_k$) for one proton. The aliphatic proton peaks were observed as a multiplate at 4.24 – 3.97 (m, $1H_l$), 3.01 – 2.83 (m, $2H_e$), 2.44 – 2.31 (m, $3H_i$) and 2.09 – 1.93 (m, $2H_f$). The mass spectrum of the compound (**275)** showed molecular ion peak at 456.34 $(M+1)^+$.

### 4.1.2.4 Synthesis of 1-(2-(1,3-dioxoisoindolin-2-yl)ethyl)piperidine-4-carboxamide (277)

1-(2-(1,3-Dioxoisoindolin-2-yl)ethyl)piperidine-4-carboxamide was synthesized using piperidine-4-carboxamide on condensation with 2-(2-bromoethyl)isoindoline-1,3-dione using DMF solvent. The synthesized compound was characterized using IR spectra i.e. carbonyl peak at 1725 $cm^{-1}$ and amide peak at 1478 $cm^{-1}$.

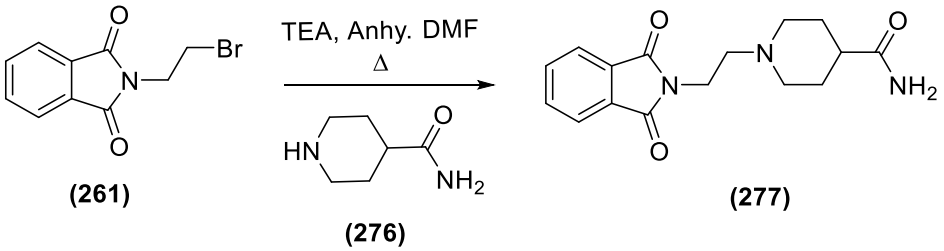


**(261)** **(276)** **(277)**

**Scheme 12**

### 4.1.2.5 Synthesis of *N*-benzyl-1-(2-(1,3-dioxoisoindolin-2-yl)ethyl)piperidine-4-carboxamide derivatives (288-297)

N-benzyl-1-(2-(1,3-dioxoisoindolin-2-yl)ethyl)piperidine-4-carboxamide derivatives was synthesized by condensation of 1-(2-(1,3-dioxoisoindolin-2-yl)ethyl)piperidine-4-carboxamide with different derivatives of benzyl bromide and benzyl chloride in the presence of anhyd. DMF and potassium carbonate. The synthesized compounds were characterized using IR, mass and NMR spectroscopy.

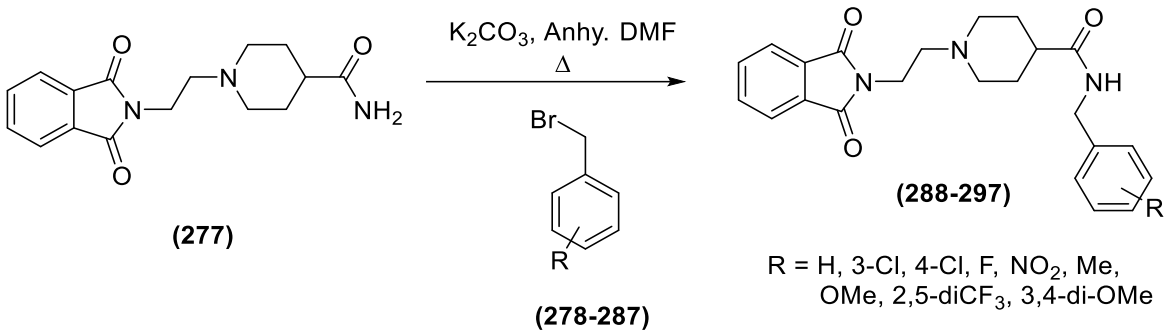


**Scheme 13**

IR spectra of compound (**288)** showed carbonyl peak at 1714 $cm^{-1}$ and amide peak at 1658 $cm^{-1}$. The PMR spectra of compound showed a multiplate peak at 8.04 – 7.94 (m, $1H_a$) for a aromatic proton, a doublet at 7.37 (d, $J$ = 4.6 Hz, $6H_{d,l,m,n,o,p}$) for six protons, a doublet over doublet at 7.30 (dd, $J$ = 5.1, 3.5 Hz, $1H_b$) and a singlet at 7.26 (s, $1H_c$). The aliphatic protons of this compound showed a singlet peak at 4.70 (s, $4H_{e,f}$) for four protons, a triplet at 3.06 (t, $J$ = 16.8 Hz, $1H_q$) for one proton, singlet at 2.95 (s, $4H_{g,i}$) for four proton along with a multiplate at 2.91 – 2.82 (m, $4H_{h,j}$) for four proton and a multiplate at 2.10 – 2.02 (m, $2H_k$) for two protons. The mass spectrum of compound (**288**) showed molecular ion peak at 393.73 (M+2).

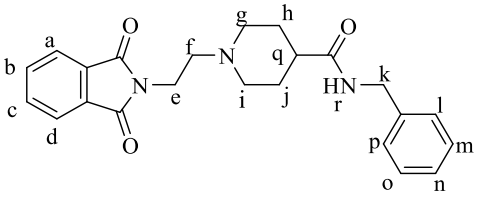

**(288)**

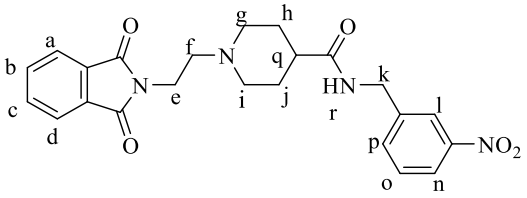


**(289)**

IR spectra of compound (**289)** showed a carbonyl peak at 1734 $cm^{-1}$ and an amide peak at 1628 $cm^{1}$. Its PMR spectra shows a singlet peak at 8.19 (s, $2H_{l,n}$) for two

protons, a doublet peak at 8.11 (d, J = 8.1 Hz, $2H_{a,d}$) for two protons, another doublet at 7.77 (d, J = 7.6 Hz, $2H_{o,p}$) for two protons. Another peak for aromatic protons were observed as a triplet at 7.63 (t, J = 7.9 Hz, $2H_{b,c}$) for two protons, as a singlet at 6.55 (s, 1H) for one proton. The aliphatic protons of compound showed a triplet at 5.54 (t, J = 5.7 Hz, $2H_k$) for two protons, a doublet at 4.64 (d, J = 5.4 Hz, $4H_{g,i}$) for four protons, a singlet at 3.33 (s, $2H_{h,j}$) for two protons. Other aliphatic proton peaks of compound were observed as a singlet at 2.70 (s, $1H_q$), as a singlet at 2.51 (s, $1H_r$), as a multiplate at 2.24 – 2.08 (m, $2H_e$), and as a multiplate at 1.36 – 1.15 (m, $2H_f$) for two protons. The mass spectra of compound (**289)** showed molecular ion peak at 437.35 $(M+1)^+$.

IR spectrum of synthesized compound (**290)** showed carbonyl peak at 1660 $cm^{-1}$ and amide peak at 1311 $cm^{-1.}$ Its PMR spectra also showed different proton peaks in aromatic and aliphatic region. For aromatic protons a singlet peak was observed at δ 8.02 (s, $1H_l$) for one proton, two doublet peaks were observed at 7.73 (d, J = 7.7 Hz, $1H_p$) and 7.65 (d, J = 7.8 Hz, $1H_a$), along with two triplet peaks at 7.59 (t, J = 7.6 Hz, $1H_d$) and 7.40 (t, J = 7.6 Hz, $1H_n$). In the aromatic region one singlet peak was also observed at 7.26 (s, $3H_{b,c,o}$) for three protons. In the aliphatic region a singlet peak was observed at 4.90 (s, $2H_k$) for two protons along with a singlet peak at 3.49 (s, $1H_q$) for one proton. For five aliphatic protons a doublet was observed at 2.92 (d, J = 29.6 Hz, $6H_{g,h,i}$), a multiplate was also observed at 2.09 (m, $4H_{e,j}$) for four protons along with a triplet at 1.26 (t, J = 9.3 Hz, $2H_f$) for two protons. The mass spectrum of compound (**290**) showed molecular ion peak at 461.78 $(M+2)^+$.

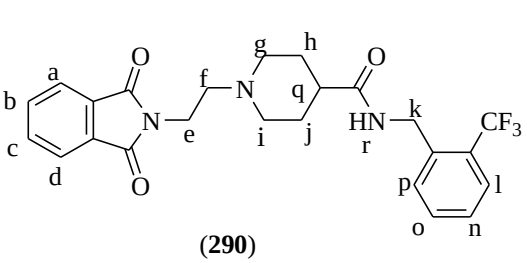


(**290**)

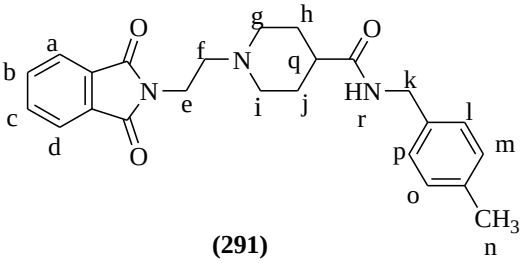


**(291)**

IR spectrum of synthesized compound (**291)** showed a carbonyl peak at 1654 $cm^{-1}$ and amide peak at 1386 $cm^{-1}$. Its PMR spectra showed a singlet peak of aromatic protons at δ 8.01 (s, $2H_{m,o}$), a doublet peak at 7.28 (d, *J* = 9.5 Hz, $3H_{a,d,p}$) for three protons and a multiplate at 7.25 – 7.13 (m, $3H_{b,c,l}$). Aliphatic protons of compound showed a doublet peak at 4.64 (d, *J* = 11.5 Hz, $2H_k$) for two protons, a singlet at 2.96 (s, $5H_{g,I,q}$) for five protons, another singlet at 2.89 (s, $4H_{h,j}$) for four protons. Similarly,

a doublet was observed at 2.72 (d, $J$ = 5.0 Hz, $2H_e$) for two protons along with a multiplate at 2.41 – 2.31 (m, $3H_n$) and a doublet at 2.08 (d, $J$ = 7.3 Hz, $2H_f$). The mass spectrum of this compound (**291**) showed a molecular ion peak at 407.66$(M+2)^+$.

IR spectrum of synthesized compound (**292)** showed a carbonyl peak at 1710 $cm^{-1}$ and amide peak at 1342 $cm^{-1}$. Its PMR spectrum showed a doublet peak at δ 8.23 (d, $J$ = 8.7 Hz, $2H_{m,o}$) for two aromatic protons, another doublet at 7.54 (d, $J$ = 8.7 Hz, $2H_{a,d}$) along with a singlet at 7.26 (s, $4H_{b,c,l,p}$) for four protons. The aliphatic protons of compound were observed as a singlet at 5.20 (s, $1H_q$), 4.85 (s, $2H_g$) and 3.49 (s, $1H_r$) for three different protons. Other aliphatic protons were observed as a doublet at 2.99 (d, J = 24.3 Hz, $2H_i$), 2.89 (s, $2H_h$) along with two singlets at 2.16 -2.10 (s, $2H_{j,}$) and 1.93 (s, $4H_{e,f}$). The mass spectrum of compound (**292**) showed molecular ion peak at 438.68 $(M+1)^+$.

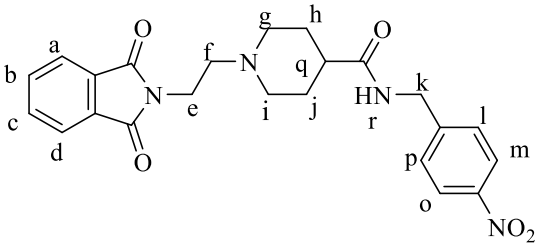


**(292)**

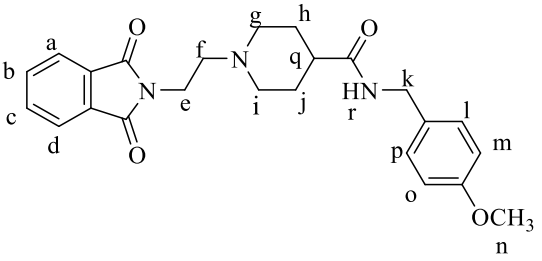


**(293)**

IR spectrum of synthesized compound (**293)** showed carbonyl peak at 1659 $cm^{-1}$ and amide peak at 1258 $cm^{-1}$. Its PMR spectra showed a multiplate peak at δ 8.20 – 7.81 (m, $1H_m$) for aromatic protons along with a multiplate at 7.35 – 7.10 (m, $2H_{a,d}$) another multiplate at 7.06 – 6.86 (m, $3H_{l,o,p}$) and 6.87 – 6.49 (m, $2H_{b,c}$). Aliphatic protons of compound showed a multiplate at 5.22 – 4.92 (m, $1H_r$) along with different multiplate at 4.81 – 4.51 (m, $2H_k$), 4.07 – 3.87 (m, $1H_q$), 3.89 – 3.63 (m, $6H_{g,i,h}$), 3.59 – 3.36 (m, $2H_j$), 3.03 – 2.81 (m, $4H_{e,f}$) and 2.20 – 1.95 (m, $3H_n$). The mass spectrum of compound (**293**) showed molecular ion peak at 422.64 $(M+1)^+$.

IR spectrum of synthesized compound (**294)** showed carbonyl peak at 1717 $cm^{-1}$ and amide peak at 1386 $cm^{-1}$. Its PMR spectra showed aromatic proton peaks as a singlet at δ 8.01 (s, $1H_l$) and as a multiplate at 7.49 – 7.14 (m, $7H_{a,b,c,d,n,o,p}$). Its aliphatic proton showed peak as a singlet at 5.08 (s, $1H_q$) and at 4.69 (s, $2H_k$). As a doublet at

3.60 (d, J = 4.2 Hz, $2H_g$) and 2.96 (d, J = 4.1 Hz, $2H_i$) along with a singlet peak at 2.88 (s, $2H_h$) and 2.70 (s, $2H_j$). Other protons appear as a doublet at 2.32 (d, J = 23.4 Hz, $2H_e$) and 2.10 (d, J = 16.5 Hz, $2H_f$). The mass spectrum of compound (**294**) showed molecular ion peak at 427.61 $(M+2)^+$.

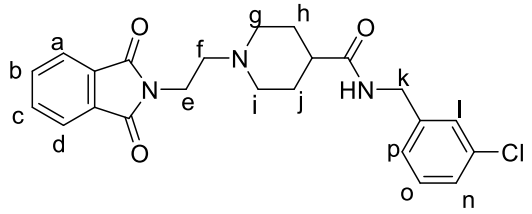


**(294)**

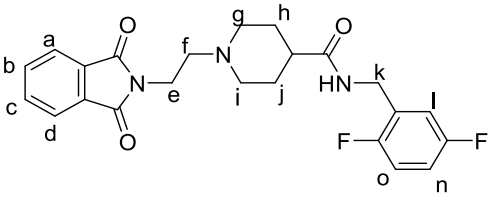


**(295)**

IR spectrum of synthesized compound (**295)** showed carbonyl peak at 1712 $cm^{-1}$ and amide peak at 1490 $cm^{-1}$. Its PMR spectra showed multiplate peak at δ 8.15 – 7.87 (m, $1H_l$), 7.37 – 7.06 (m, $3H_{a,n,o}$) and 7.12 – 6.78 (m, $3H_{b,c,d}$). Its aliphatic protons showed a doublet over doublet peak at 5.30 (dd, *J* = 26.2, 15.0 Hz, $1H_q$), a doublet at 4.70 (d, *J* = 39.0 Hz, $2H_k$), a multiplate at 4.00 – 3.74 (m, $2H_g$). Its proton also shows a triplet peak at 2.95 (t, *J* = 25.2 Hz, $4H_{i,h}$), a multiplate at 2.84 – 2.54 (m, $2H_j$), 2.60 – 2.21 (m, $2H_e$) and 2.18 – 1.90 (m, $2H_f$). The mass spectrum of compound (**295**) showed molecular ion peak at 429.47 $(M+2)^+$.

IR spectrum of synthesized compound (**296)** showed carbonyl peak at 1711 $cm^{-1}$ and amide peak at 1217 $cm^{-1}$. Its PMR spectrum showed aromatic proton peak at 8.13 – 7.92 (m, $1H_m$) as a multiplate, at 7.40 – 7.30 (m, $2H_{n,a}$) as a multiplate for two protons, at 7.26 (s, $3H_{d,l,o}$ ) as a singlet for three protons and at 7.11 – 6.98 (m, $2H_{b,c}$) as a multiplate for two protons. The aliphatic proton peaks of compound were observed as a doublet at 4.69 (d, J = 17.5 Hz, $2H_k$), as a multiplate at 3.94 – 3.84 (m, $1H_q$), another multiplate at 3.64 – 3.45 (m, $2H_g$), a doublet over doublet at 2.95 (dd, J = 28.9, 19.7 Hz, $4H_{i,h}$), as a multiplate at 2.18 – 2.05 (m, $2H_j$) and as a singlet at 1.93 (s, $4H_{e,f}$) for four protons. The mass spectrum of compound (**296**) showed molecular ion peak at 411.56 $(M+2)^+$.

IR spectrum of synthesized compound (**297)** showed carbonyl group peak at 1713 $cm^{-1}$ and amide group peak at 1491 $cm^{-1}$. Its PMR spectra showed aromatic proton peak at δ 8.07 – 7.81 (m, $1H_m$) as a multiplate and an another multiplate at 7.40 – 7.20 (m, $7H_{a,b,c,d,l,n,o}$). The aliphatic protons showed a singlet peak at 4.68 (s, $2H_k$), a

multiplate peak at 3.98 – 3.76 (m, $1H_q$), another multiplate at 3.60 – 3.38 (m, $2H_g$), a doublet over doublet at 2.96 (dd, J = 41.3, 30.7 Hz, $4H_{e,f}$) and a multiplate at 2.23 – 1.96 (m, $6H_{h,j,i}$). The mass spectrum of compound (**297**) showed molecular ion peak at 427.52 $(M+2)^+$.

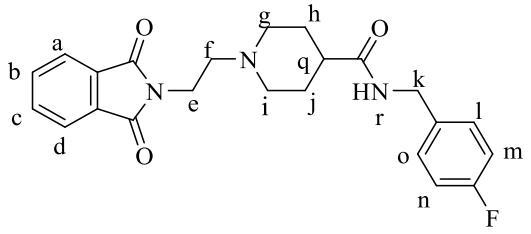

**(296)**

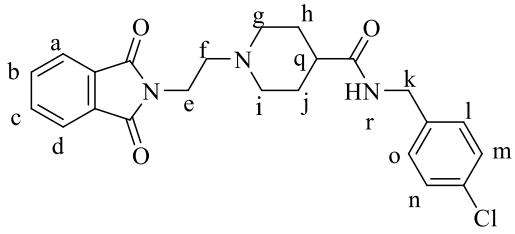

**(297)**

## 4.2 Biological screening

### 4.2.1 Biological evaluation of synthesized compounds (186-224, 263-275 and 288-297)

The synthesized derivatives were screened against 3D7 strain of *Plasmodium falciparum* with different concentration (**Table 5)** compared with standard drug chloroquine that has shown 94.8% at 25nM concentration**.** A primary *in vitro* screening of the synthesized compounds was conducted at three different concentrations: 50nM, 500nM and 10µM against the 3D7 of *Plasmodium falciparum*. Counting of Giemsa-stained smears[18] revealed that the compounds (**189, 190, 198**, **209**, **270, 272-274, 289-296)** showed inhibition even at the 50nM concentration.

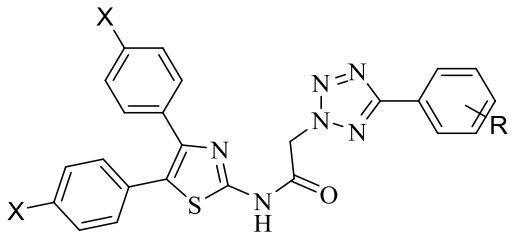

**(186-224)**

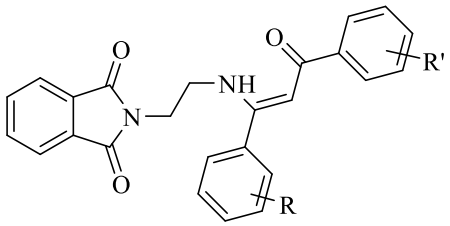

**(263 - 275)**

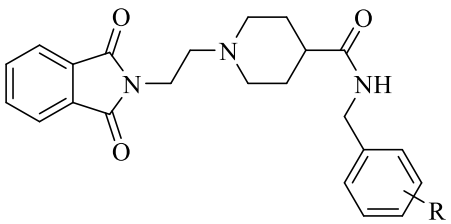

**(288 - 297)**

**Table 5**: *In vitro* anti-malarial activity (% inhibition) of synthesized compounds at varying concentrations **(186-224, 266-275** and **288-297)**

| Comp ID | X | R | 10uM | 500nM | 50nM |
|---|---|---|---|---|---|
| **186** | H | OH | 97.71 | 4.28 | 0 |
| **187** | H | 4-$OCH_3$ | 97.14 | 4.28 | 0 |
| **188** | H | 3-Cl | 0 | 0 | 0 |
| **189** | H | 4-Br | 12.85 | 7.14 | 4.28 |
| **190** | H | 3-$NO_2$ | 18.57 | 5.71 | 4.28 |
| **191** | H | 4-$CH_3$ | 64.28 | 4.28 | 0 |
| **192** | H | H | 4.28 | 0 | 0 |
| **193** | H | 3-$CH_3$ | 8.75 | 5 | 0 |
| **194** | H | 3-$OCH_3$ | 6.5 | 1.25 | 5 |
| **195** | H | 2-$NO_2$ | 28.75 | 6.25 | 0 |
| **196** | H | 3-Br | 16.25 | 0 | 0 |
| **197** | H | 4-*i*Pr | 22.5 | 0 | 0 |
| **198** | H | 4-F | 92.75 | 77.62 | 6.25 |
| **199** | Cl | 3,4-Di$OCH_3$ | 8.57 | 0 | 0 |
| **200** | Cl | OH | 87 | 22.37 | 0 |
| **201** | Cl | 4-$OCH_3$ | 4.28 | 0 | 0 |
| **202** | Cl | 3-Cl | 4.28 | 1.42 | 0 |
| **203** | Cl | 4-Br | 97.71 | 0 | 0 |
| **204** | Cl | 3-$NO_2$ | 48.57 | 10 | 0 |
| **205** | Cl | 4-$CH_3$ | 36.25 | 0 | 0 |
| **206** | Cl | H | 96.875 | 0 | 0 |
| **207** | Cl | 3-$CH_3$ | 89.62 | 0 | 0 |
| **208** | Cl | 3-$OCH_3$ | 4.28 | 0 | 0 |
| **209** | Cl | 2-$NO_2$ | 90.42 | 11.42 | 8.57 |
| **210** | Cl | 3-Br | 97.14 | 40 | 0 |
| **211** | Cl | 4-*i*Pr | 10.18 | 2.82 | 0 |
| **212** | Cl | 4-F | 36.25 | 11.25 | 0 |
| **213** | $OCH_3$ | 3,4-Di$OCH_3$ | 4.28 | 4.28 | 0 |
| **214** | $OCH_3$ | OH | 20 | 0 | 0 |
| **215** | $OCH_3$ | 4-$OCH_3$ | 50 | 50 | 0 |
| **216** | $OCH_3$ | 3-Cl | 16.25 | 0 | 0 |
| **217** | $OCH_3$ | 4-Br | 21.42 | 4.28 | 0 |
| **218** | $OCH_3$ | 3-$NO_2$ | 67.14 | 44.28 | 0 |

| | | | | | |
|---|---|---|---|---|---|
| **219** | $OCH_3$ | 4-$CH_3$ | 74.28 | 50 | 18.57 |
| **220** | $OCH_3$ | H | 47.14 | 17.14 | 17.14 |
| **221** | $OCH_3$ | 3-$CH_3$ | 40 | 5 | 0 |
| **222** | $OCH_3$ | 3-$OCH_3$ | 41.25 | 0 | 0 |
| **223** | $OCH_3$ | 2-$NO_2$ | 0 | 0 | 0 |
| **224** | $OCH_3$ | 4-F | 11.42 | 7.14 | 0 |
| **263** | F | - | 2.5 | 0 | 0 |
| **264** | - | $CH_3$ | 30 | 7.14 | 0 |
| **265** | OH | - | 0 | 0 | 0 |
| **266** | $NH_2$ | - | 0 | 0 | 0 |
| **268** | OH | $CH_3$ | 0 | 0 | 0 |
| **269** | OH | 3-Br | 0 | 0 | 0 |
| **270** | Cl | 3-$NO_2$ | 83.75 | 2.5 | 0 |
| **272** | 4-F | 4-F | 100 | 11.25 | 0 |
| **273** | $CH_3$ | 4-F | 98 | 58.75 | 13.75 |
| **274** | $NO_2$ | Cl | 97.14 | 17.71 | 0 |
| **275** | $NO_2$ | OH | 0 | 0 | 0 |
| **288** | H | - | 0 | 0 | 0 |
| **289** | 3-$NO_2$ | - | 83.75 | 66.25 | 62.5 |
| **290** | 2-$CF_3$ | - | 97.14 | 42.85 | 42.85 |
| **291** | 4-$CH_3$ | - | 97.14 | 1.42 | 0 |
| **292** | 4-$NO_2$ | - | 87.87 | 65 | 27.5 |
| **293** | 3-$OCH_3$ | - | 84.12 | 82.12 | 76.62 |
| **294** | 3-Cl | - | 15 | 3.75 | 10 |
| **295** | 3,6-Difluoro | - | 95.71 | 54.28 | 50 |
| **296** | 4-F | - | 20 | 5 | 0 |
| **297** | 4-Cl | - | 7.5 | 0 | 0 |

A comprehensive evaluation of the *in vitro* antiplasmodial activity of the synthesized compounds (**186–224**) is depicted in **Fig. 4.1. S**everal compounds, including (**186, 187, 198, 203, 204** and **207)**, showed strong inhibition at 10 μM but lost potency at lower concentrations, indicating limitations in permeability or metabolic stability. In contrast, compounds (**198, 217, 218** and **219)** retained substantial activity at nanomolar levels, suggesting favorable pharmacokinetic properties and strong target engagement. A subset of derivatives **(190–194, 210, 211, 223, 224)** remained inactive,

likely due to poor physicochemical profiles or steric hindrance. Notably, compounds **(216)** and **(220)** exhibited moderate but consistent inhibition across all concentrations, supporting their potential for further optimization.

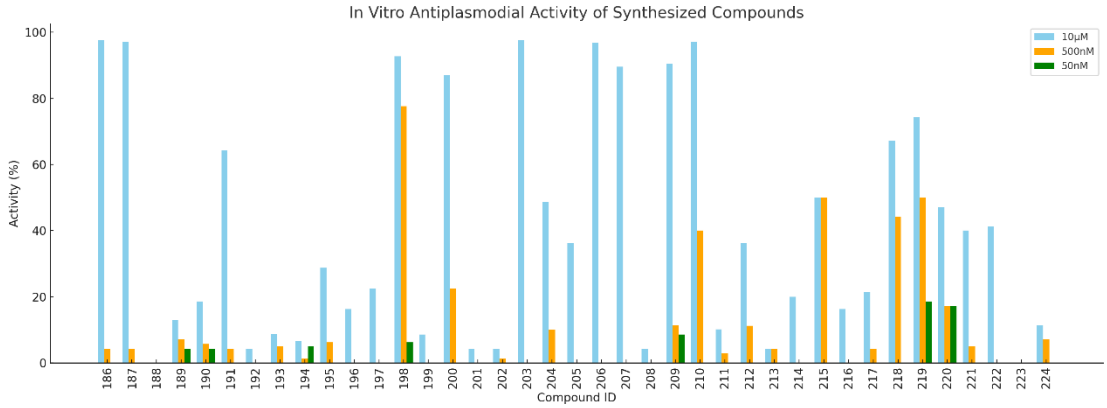


**Fig. 4.1** Concentration-dependent *in vitro* antimalarial activity of synthesized compounds **(186-224)** against *P. falciparum*

A detailed evaluation of the *in vitro* antiplasmodial activity of isoindoline-1,3-dione derivatives (compounds **263–275** and **288-297**) is presented in **Fig. 4.2**, highlighting their concentration-dependent efficacy at 10 μM, 500 nM, and 50 nM.

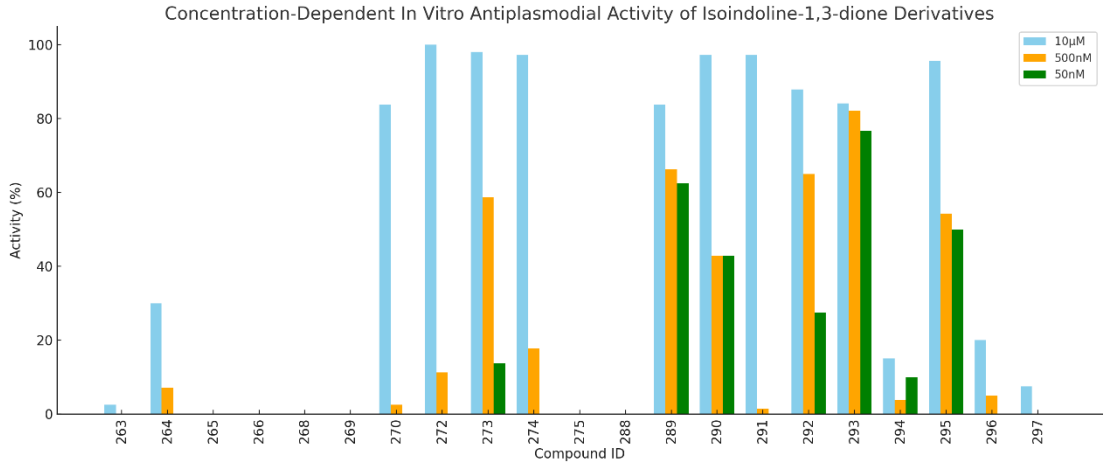


**Fig. 4.2** Concentration-dependent *in vitro* antimalarial activity of synthesized compounds (**263-275** and **288-297**) against *Plasmodium falciparum*

A detailed evaluation of the *in vitro* antiplasmodial activity of isoindoline-1,3-dione derivatives (**263–275** and **288-297**) is presented in **Fig. 4.2**, highlighting their concentration-dependent efficacy at 10 μM, 500 nM, and 50 nM. While several compounds exhibited strong inhibitory effects at 10 μM, only a few retained activities at lower concentrations, indicating significant structure–activity relationship (SAR) implications. Compounds **(270, 272** and **274)** showed high activity at 10 μM but a

marked reduction at 500 nM and complete loss at 50 nM, suggesting limited potency or poor cell permeability at submicromolar levels. In contrast, compounds **(273, 290, 293** and **295**) maintained substantial activity at 500 nM and 50 nM. Notably, compound **(293)** demonstrated potent inhibition across all concentrations (84.1%, 82.1%, and 76.6%), indicating favourable pharmacokinetic properties and strong target affinity. Compound **(290)** also displayed consistent efficacy (97.1%, 42.9%, and 42.9%), making it a promising lead for further optimization. Compound **(294),** though not highly potent at 10 μM, exhibited stable activity (15%, 3.75%, 10%) across all concentrations, suggesting potential for sustained action at lower doses, possibly due to stable receptor binding or enhanced bioavailability. In contrast, compounds **(265, 266, 268,** and **269)** were inactive across all concentrations. Their lack of activity may result from excessive polarity or steric hindrance introduced by their substituents.

### 4.3 Computational studies

Molecular docking and ADMET predication studies of the synthesized compounds were carried out to assess their potential as bioactive agents. Molecular docking studies provided insights into the binding interactions between the synthesized compounds and the target protein, revealing key binding affinities and molecular interactions such as hydrogen bonding, hydrophobic interactions, and π-π stacking etc**.**

ADMET analysis was performed to predict the pharmacokinetic properties, including absorption, distribution, metabolism, excretion, and toxicity, ensuring the drug-like potential of the compounds. These properties were compared against standard reference compound chloroquine to evaluate their suitability for further drug development.

#### 4.3.1 Molecular docking studies of synthesized derivatives

To rationalize the observed antimalarial activity and explore potential binding interactions, molecular docking studies were performed for the most potent compounds using the *Plasmodium falciparum* dihydrofolate reductase-thymidylate synthase (PfDHFR-TS) crystal structure (PDB ID: 2GHU). Docking was carried out using Schrodinger software to evaluate the binding affinity and orientation of the ligands within the active site. Based on biological screening, compounds (**219, 220, 289, 290** and **293)**, which demonstrated potent inhibition at concentrations as low as 50 nM, were selected for detailed docking analysis **(Table 6).** These studies aimed to elucidate key

molecular interactions responsible for the high binding affinity and to identify structure-activity correlations consistent with the biological data. To ensure the accuracy of the docking methodology, the co-crystallized ligand was redocked into the active site of protein The obtained root-mean-square deviation (RMSD) value of 0.28 Å confirmed the reliability of the docking protocol.

**Table 6**: Binding affinities of synthesized compounds against *Pf*DHFR-TS **(186-224, 263-275** and **288-297)**

| Comp ID | Binding affinity (kcal/mol) | Comp ID | Binding affinity (kcal/mol) |
|---|---|---|---|
| **186** | -6.71 | **219** | -7.94 |
| **187** | -6.82 | **220** | -7.80 |
| **188** | -6.01 | **221** | -6.87 |
| **189** | -6.23 | **222** | -5.64 |
| **190** | -6.04 | **223** | -6.31 |
| **191** | -5.74 | **224** | -5.79 |
| **192** | -6.03 | **263** | -6.47 |
| **193** | -5.95 | **264** | -5.26 |
| **194** | -7.01 | **265** | -6.52 |
| **195** | -6.31 | **266** | -5.62 |
| **196** | -5.44 | **267** | -5.67 |
| **197** | -5.47 | **268** | -6.54 |
| **198** | -7.08 | **269** | -6.39 |
| **199** | -6.58 | **270** | -6.71 |
| **200** | -6.99 | **271** | -4.92 |
| **201** | -6.21 | **272** | -6.92 |
| **202** | -5.90 | **273** | -5.11 |
| **203** | -6.04 | **274** | -5.26 |
| **204** | -5.87 | **275** | -5.74 |
| **205** | -5.86 | **288** | -8.16 |
| **206** | -4.99 | **289** | -7.88 |
| **207** | -6.48 | **290** | -8.02 |
| **208** | -6.64 | **291** | -6.11 |
| **209** | -5.93 | **292** | -7.05 |
| **210** | -5.67 | **293** | -7.97 |
| **211** | -5.18 | **294** | -7.07 |
| **212** | -5.54 | **295** | -7.52 |
| **213** | -6.97 | **296** | -6.51 |
| **214** | -6.19 | **297** | -7.66 |
| **215** | -7.00 | **Chloroquine** | -6.24 |
| **216** | -5.50 | | |
| **217** | -5.97 | | |
| **218** | -5.74 | | |

The docking analysis of the standard chloroquine with *Pf*DHFR-TS **(Fig 4.3)** reveals strong binding through key hydrogen bonds with Asp35, Gln36, and His174, as well as hydrophobic interactions with Trp206 and Trp210. The chlorinated aromatic ring contributes to π–π stacking, while van der Waals contacts with residues like Ala157 and Val152 enhance binding stability. The thioether linker offers conformational flexibility, allowing optimal occupation of the binding pocket.

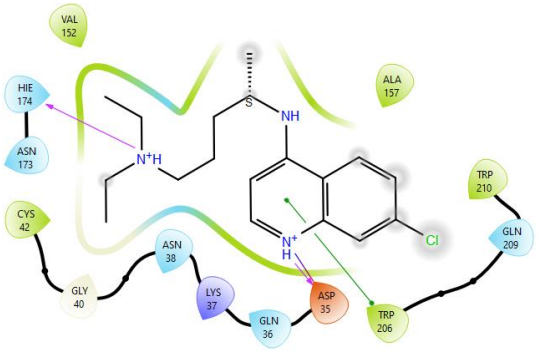


**Fig. 4.3** 2D interactions of chloroquine within the active site of *Pf*DHFR-TS receptor

The docking analyses of these two compounds **(219-220)** with *Pf*DHFR-TS **(Fig. 4.4 a, b)** revealed strong and complementary binding interactions, underscoring their potential as effective enzyme inhibitors. Both compounds form key hydrogen bonds with residues such as Lys37, Asn38, and Cys42, and engage in π–π stacking with Trp206, which together contribute to stable binding within the active site.

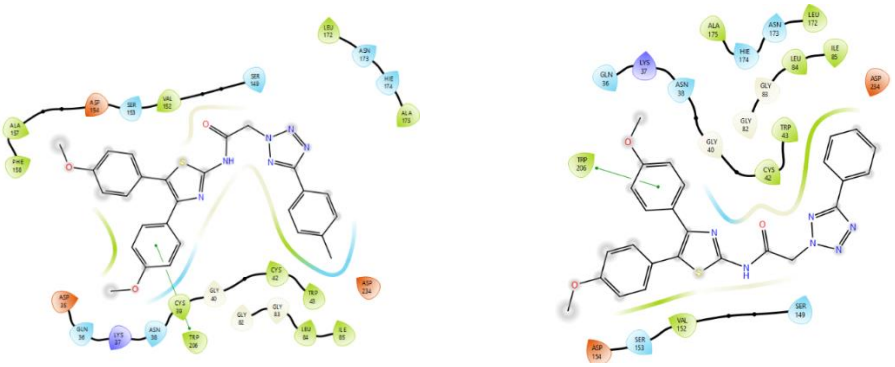

(a) (b)

**Fig. 4.4** 2D interactions of (a) compound (**219)** and (b) compound (**220)** within the active site of *Pf*DHFR-TS

Hydrophobic contacts with Val152, Leu84, and Ile85 further reinforce affinity. However, distinct differences in their interaction profiles are evident.

The docking analysis of compound **(289)** revealed a favourable binding conformation characterized by a salt bridge with Asp234 and hydrogen bonding with

Asn173 and Lys37 as shown in **(Fig. 4.5 a).** The ligand is additionally stabilized through hydrophobic contacts involving Ile85, Leu84, and aromatic interactions with Trp43, contributing to its firm placement within the binding pocket. Compound (**290**) exhibited a distinct interaction profile, forming hydrogen bonds with Asn38, Gln171, and Asn173. A π–π interaction with Trp43, along with van der Waals contacts involving residues like Ala157 and Val152, further strengthened the binding (**Fig. 4.5 b**). The trifluoromethyl group was well accommodated within a hydrophobic region, enhancing ligand affinity. Similarly for compound (**293**), key interactions included hydrogen bonding with Asn86, Asn173, and Gln171, along with polar contact to Leu172 (**Fig. 4.5 (c)**).The ligand also formed stabilizing interactions with Leu84 and Ile85. A supportive hydrophobic environment created by Trp43, Cys42, and Val152 aided in securing the ligand within the active site.

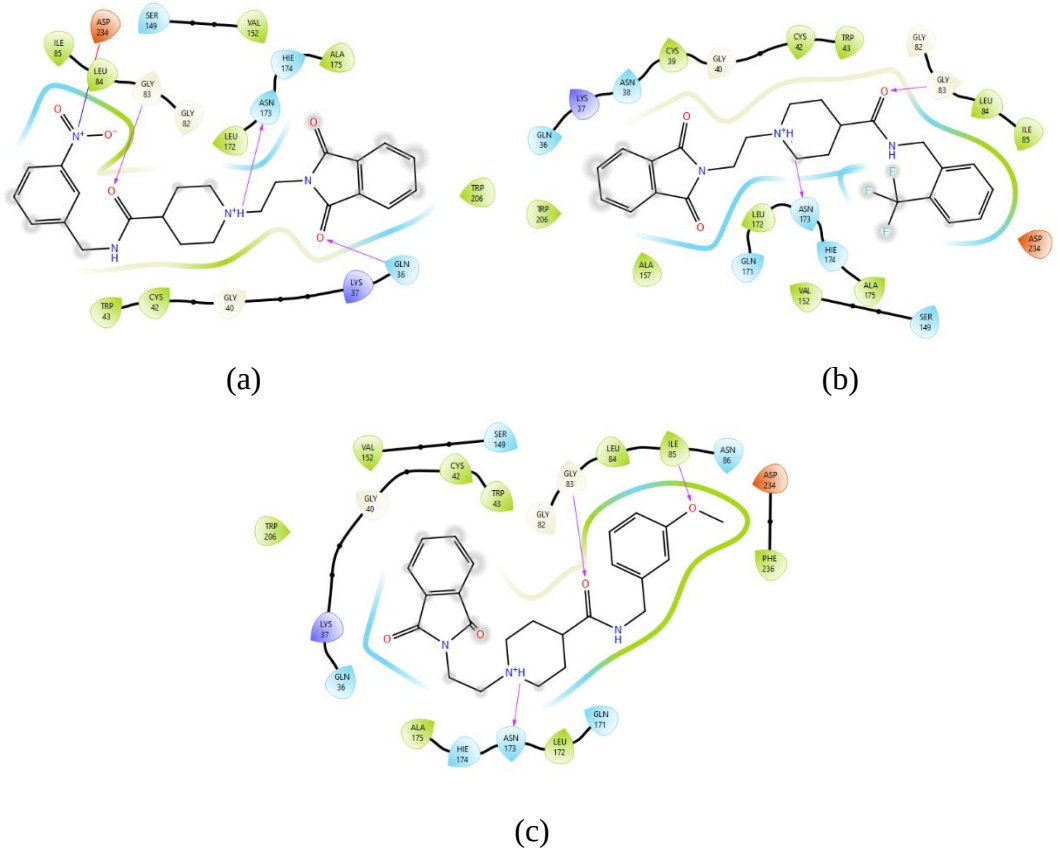

(a) (b)

(c)

**Fig. 4.5** 2D interactions of compound (a) **289** and (b) **290** (c) **293** within the active site of *Pf*DHFR-TS

The docking results highlighted the significance of hydrogen bonding, π-π stacking, and Van der Waals forces in stabilizing the compounds within the active site of *Pf*DHFR-TS. The presence of functional groups such as hydroxyl, carbonyl, and

aromatic rings facilitated strong interactions with key residues, particularly Cys42, His174, and Asn77, which are crucial for enzymatic activity. When the docking studies compared with standard drug Chloroquine, a well-known antimalarial drug, was also docked against *Pf*DHFR-TS to assess its binding interactions and compare its inhibitory potential with the synthesized compounds. The docking score of chloroquine was recorded at -6.24 kcal/mol, indicating a moderate binding affinity.

Furthermore, the potential dual-action mechanism of these compounds, targeting both *Pf*DHFR-TS and hemozoin formation disruption, suggests an enhanced antimalarial efficacy. This mechanism could reduce the likelihood of resistance development, making these compounds valuable candidates for further investigation. The molecular docking study demonstrated that the synthesized compounds exhibit promising inhibitory potential against *Pf*DHFR-TS, with compound (**290)** emerging as the most potent candidate. The strong binding interactions observed reinforce their potential as novel antimalarial agents.

### 4.3.2 *In-silico* prediction of physicochemical and pharmacokinetic parameters of the synthesized compounds (186-224, 263-275 and 288-297)

Absorption, Distribution, Metabolism, and Excretion (ADME) predictions were carried out for the synthesized compounds using chloroquine and artemisinin as reference drugs (**Table 7**). The evaluation was based on key pharmacokinetic and physicochemical parameters, including partition coefficient (QlogPo/w), aqueous solubility (QlogS), blood-brain barrier permeability (QlogBB)[13], polar surface area (PSA), and compliance with Lipinski's Rule of Five (RO5)[13].

The designed compounds demonstrated high lipophilicity, with QlogPo/w values exceeding 5, which generally enhances membrane permeability and blood-brain barrier (BBB) penetration[14-15]. Furthermore, the high polar surface area (PSA) values suggest limited passive membrane permeability, which may restrict oral absorption[16] (**Table 7).**

**Table 7.** Predicted pharmacokinetic properties of synthesized compounds **(186-224, 263-275** and **288-297)**

| Comp | MW | HBD | HBA | Rule of 5 | QPlogPo/w | BBB permeation | GI absorption | logS | PSA |
|---|---|---|---|---|---|---|---|---|---|
| **186** | 454.12 | 2 | 6 | 0 | 3.09 | No | Low | -6.05 | 134.06 |
| **187** | 468.14 | 1 | 6 | 0 | 3.15 | No | Low | -6.26 | 123.06 |
| **188** | 472.09 | 1 | 5 | 0 | 3.74 | No | Low | -6.78 | 113.83 |
| **189** | 517.40 | 1 | 5 | 1 | 3.87 | No | Low | -7.10 | 113.83 |
| **190** | 483.11 | 1 | 7 | 0 | 2.63 | No | Low | -6.24 | 159.65 |
| **191** | 452.14 | 1 | 5 | 0 | 3.25 | No | Low | -6.49 | 113.83 |
| **192** | 438.50 | 1 | 5 | 0 | 3.48 | No | Low | -6.19 | 113.83 |
| **193** | 452.14 | 1 | 5 | 0 | 3.66 | No | Low | -6.49 | 113.83 |
| **194** | 468.14 | 1 | 6 | 0 | 3.73 | No | Low | -6.26 | 123.06 |
| **195** | 483.11 | 1 | 7 | 0 | 2.72 | No | Low | -6.24 | 159.65 |
| **196** | 517.40 | 1 | 5 | 1 | 3.91 | No | Low | -7.10 | 113.83 |
| **197** | 480.17 | 1 | 5 | 0 | 4.09 | No | Low | -7.04 | 113.83 |
| **198** | 456.12 | 1 | 6 | 0 | 3.44 | No | Low | -6.35 | 113.83 |
| **199** | 567.45 | 1 | 7 | 1 | 4.48 | No | Low | -7.51 | 132.29 |
| **200** | 523.39 | 2 | 6 | 1 | 3.33 | No | low | -7.23 | 134.06 |
| **201** | 537.42 | 1 | 6 | 1 | 4.13 | No | Low | -7.44 | 123.06 |
| **202** | 541.84 | 1 | 5 | 2 | 4.23 | No | Low | -7.97 | 113.83 |
| **203** | 586.29 | 1 | 5 | 2 | 3.92 | No | Low | -8.28 | 113.83 |
| **204** | 552.39 | 1 | 7 | 1 | 3.07 | No | Low | -7.43 | 159.65 |
| **205** | 521.42 | 1 | 5 | 1 | 3.34 | No | Low | -7.67 | 113.83 |
| **206** | 507.39 | 1 | 5 | 1 | 3.59 | No | Low | -7.37 | 113.83 |
| **207** | 521.42 | 1 | 5 | 1 | 3.94 | No | Low | -7.48 | 113.83 |
| **208** | 537.42 | 1 | 6 | 1 | 4.13 | No | Low | -7.44 | 123.06 |
| **209** | 552.39 | 1 | 7 | 1 | 3.21 | No | Low | -7.43 | 159.65 |
| **210** | 586.29 | 1 | 5 | 2 | 4.16 | No | Low | -8.28 | 113.83 |
| **211** | 549.47 | 1 | 5 | 2 | 4.16 | No | Low | -8.23 | 113.83 |
| **212** | 525.38 | 1 | 6 | 2 | 3.45 | No | Low | -7.53 | 113.83 |
| **213** | 558.61 | 1 | 9 | 2 | 3.77 | No | low | -6.47 | 150.75 |
| **214** | 514.56 | 2 | 8 | 1 | 3.85 | No | Low | -6.18 | 152.52 |
| **215** | 528.59 | 1 | 8 | 1 | 3.80 | No | Low | -6.40 | 141.52 |
| **216** | 533.00 | 1 | 7 | 1 | 4.41 | No | Low | -6.92 | 132.29 |
| **217** | 577.46 | 1 | 7 | 1 | 4.41 | No | Low | -7.24 | 132.29 |
| **218** | 543.56 | 1 | 9 | 2 | 3.38 | No | Low | -6.39 | 152.37 |
| **219** | 512.59 | 1 | 7 | 1 | 4.39 | No | Low | -6.63 | 132.29 |
| **220** | 498.56 | 1 | 7 | 0 | 4.13 | No | Low | -6.33 | 132.29 |
| **221** | 512.59 | 1 | 7 | 1 | 4.04 | No | Low | -6.63 | 132.29 |

| | | | | | | | | | |
|---|---|---|---|---|---|---|---|---|---|
| **222** | 528.55 | 1 | 8 | 1 | 4.01 | No | low | -6.40 | 141.52 |
| **223** | 543.56 | 1 | 9 | 2 | 3.21 | No | Low | -6.39 | 152.37 |
| **224** | 516.55 | 1 | 8 | 1 | 4.31 | No | Low | -6.49 | 132.29 |
| **263** | 410.46 | 1 | 3 | 0 | 3.46 | Yes | High | -5.54 | 66.48 |
| **264** | 412.44 | 2 | 4 | 0 | 2.96 | No | High | -5.10 | 86.71 |
| **265** | 411.45 | 2 | 3 | 0 | 3.07 | No | High | -4.88 | 92.50 |
| **266** | 412.44 | 2 | 4 | 0 | 2.95 | No | High | -5.10 | 86.71 |
| **267** | 411.45 | 2 | 3 | 0 | 3.07 | No | High | -4.88 | 92.50 |
| **268** | 426.46 | 2 | 4 | 0 | 2.84 | No | High | -5.40 | 86.71 |
| **269** | 491.33 | 2 | 4 | 0 | 3.08 | No | High | -6.01 | 86.71 |
| **270** | 475.88 | 1 | 5 | 0 | 3.39 | No | High | -5.90 | 112.30 |
| **271** | 509.78 | 1 | 3 | 2 | 3.67 | Yes | High | -6.74 | 66.48 |
| **272** | 432.42 | 1 | 5 | 0 | 3.15 | Yes | High | -5.56 | 66.48 |
| **273** | 448.87 | 1 | 4 | 0 | 3.18 | Yes | High | -5.90 | 66.48 |
| **274** | 475.88 | 1 | 5 | 0 | 3.29 | Yes | High | -5.90 | 112.30 |
| **275** | 455.46 | 1 | 5 | 0 | 3.30 | Yes | High | -5.60 | 112.30 |
| **288** | 391.46 | 1 | 4 | 0 | 3.21 | Yes | High | -3.50 | 69.72 |
| **289** | 436.46 | 1 | 6 | 0 | 2.78 | No | High | -3.57 | 115.54 |
| **290** | 459.46 | 1 | 7 | 0 | 3.48 | Yes | High | -4.38 | 69.72 |
| **291** | 405.49 | 1 | 4 | 0 | 3.42 | Yes | High | -3.81 | 69.72 |
| **292** | 436.46 | 1 | 6 | 0 | 2.85 | No | High | -3.57 | 115.54 |
| **293** | 421.49 | 1 | 5 | 0 | 3.37 | No | High | -3.58 | 78.95 |
| **294** | 425.91 | 1 | 4 | 0 | 3.40 | Yes | High | -4.10 | 69.72 |
| **295** | 427.44 | 1 | 6 | 0 | 3.27 | Yes | High | -3.83 | 69.72 |
| **296** | 409.45 | 1 | 5 | 0 | 3.24 | Yes | High | -3.66 | 69.72 |
| **297** | 425.91 | 1 | 4 | 0 | 3.38 | Yes | High | -4.10 | 69.72 |
| **Chloroquine** | 319.87 | 2 | 3 | 0 | 4.4 | Yes | High | 4.10 | 28.16 |

Rule of 5: Lipinski Rule of 5; MW: Molecular Weight; HBD: Hydrogen Bond Donor; HBA: Hydrogen Bond Acceptor; QPlogPo/w: predicted octanol/water partition coefficient; BBB: blood brain partition; PSA: Polar Surface area; #Star: number of parameters with values that fall outside the 95% range of similar values for known drugs[17]

Among the synthesized compounds, some of the compounds (**263, 271-275**, **288, 290, 291, 294-297**) exhibited pharmacokinetic properties similar to antimalarial drugs chloroquine. These compounds share key characteristics such as moderate molecular weight (ranging from 391.46 to 509.78 Da), compliance with Lipinski's Rule of 5, and optimal lipophilicity. All these compounds demonstrate high gastrointestinal (GI) absorption, ensuring good oral bioavailability. Additionally, several of these compounds (**263**, **271-275**) show blood-brain barrier (BBB) permeation, a property that can be relevant for antimalarial drugs targeting cerebral malaria. Their aqueous solubility (logS values between -6.74 and -3.50) is within a reasonable range for drug-

like properties, while their polar surface area (PSA) remains under 120 Å², supporting effective permeability. These favorable pharmacokinetic traits suggest their potential as promising candidates for further antimalarial drug development.

### 4.3.3 Toxicity prediction of synthesized compounds (186-224)

Derek Nexus is a structure-based toxicity prediction tool that evaluates potential toxicological risks by analyzing chemical structures against a database of known toxophores. It provides toxicity predictions based on its knowledge-based reasoning, making it a valuable tool for early-stage compound screening. For toxicity predication Derek system identifies structural alerts by comparing a compound's structure to a database of known toxicophores associated with toxicity. Whereas Sarah system provides quantitative probability-based assessments for toxicity, by using a large dataset of Ames test results to predict mutagenicity.

*In silico* toxicity assessment using derek nexus indicated that approximately 95% of the 62 compounds were classified as "Inactive", suggesting a low likelihood of toxicity based on known structural alerts **(Table 6)**. Notably, some compounds were flagged as "Plausible", indicating the potential presence of structural features that may be associated with toxicity under specific biological conditions. Complementary predictions from sarah nexus, which focuses on mutagenicity potential, identified only seven compounds as negative, consistent with derek's assessment. Additionally, three compounds (**204, 218** and **223**) were classified as "Outside Domain" by Sarah, indicating that their chemical structures fall beyond the applicability domain of the model, likely due to structural novelty or complexity

**Table 6** Toxicity assessment of synthesized compounds **(186-224)** using Derek nexus

| Comp ID | Predication by Derek | Predication by Sarah | Comp ID | Predication by Derek | Predication by Sarah |
|---|---|---|---|---|---|
| **186** | Inactive | Positive | **219** | Inactive | Positive |
| **187** | Inactive | Positive | **220** | Inactive | Positive |
| **188** | Inactive | Equivocal | **221** | Inactive | Positive |
| **189** | Inactive | Positive | **222** | Inactive | Positive |
| **190** | Plausible | Positive | **223** | Inactive | Outside domain |
| **191** | Inactive | Equivocal | **224** | Inactive | Positive |
| **192** | Inactive | Equivocal | **263** | Inactive | Equivocal |
| **193** | Inactive | Equivocal | **264** | Inactive | Equivocal |
| **194** | Inactive | Positive | **265** | Inactive | Equivocal |

| | | | | | |
|---|---|---|---|---|---|
| **195** | Plausible | Positive | **266** | Inactive | Equivocal |
| **196** | Inactive | Positive | **267** | Inactive | Equivocal |
| **197** | Inactive | Negative | **268** | Inactive | Negative |
| **198** | Inactive | Equivocal | **269** | Inactive | Positive |
| **199** | Inactive | Positive | **270** | Inactive | Positive |
| **200** | Inactive | Positive | **271** | Inactive | Positive |
| **201** | Inactive | Positive | **272** | Inactive | Equivocal |
| **202** | Inactive | Positive | **273** | Inactive | Negative |
| **203** | Inactive | Positive | **274** | Inactive | Negative |
| **204** | Inactive | Outside domain | **275** | Inactive | Negative |
| **205** | Inactive | Positive | **288** | Inactive | Positive |
| **206** | Inactive | Positive | **289** | Inactive | Negative |
| **207** | Inactive | Positive | **290** | Inactive | Equivocal |
| **208** | Inactive | Positive | **291** | Inactive | Negative |
| **209** | Plausible | Positive | **292** | Inactive | Positive |
| **210** | Inactive | Equivocal | **293** | Inactive | Positive |
| **211** | Inactive | Negative | **294** | Inactive | Equivocal |
| **212** | Inactive | Equivocal | **295** | Inactive | Equivocal |
| **213** | Inactive | Positive | **296** | Inactive | Positive |
| **214** | Inactive | Positive | **297** | Inactive | Equivocal |
| **215** | Inactive | Positive | **Chloroquine** | Inactive | Equivocal |
| **216** | Inactive | Positive | | | |
| **217** | Inactive | Positive | | | |
| **218** | Inactive | Outside domain | | | |

### 4.3.4 Structure activity relationship studies

From the biological data the structure activity relationship (SAR) of vicinal diaryl fused tetrazole compounds **(186-224**) were established and discussed as follows:

SAR analysis of the given vicinal diaryl based tetrazolyl-thiazole derivatives provides insights into the effects of various functional groups on biological activity at 50nM concentration. This section systematically examines how specific structural modifications impacted the potency of compounds **(Fig. 4.6).**

- **Effect of halogen substitutions**

Halogen substitutions showed a significant influence on activity, with bromine and fluorine showing favourable effects. The 4-bromophenyl (**189**) and 3-bromophenyl (**196**) substitutions exhibit moderate to high activity, suggesting that bromine at these positions enhances target interactions. The fluorine-substituted compound (**198**) also

maintains reasonable potency, due to its strong electronegativity and hydrogen bond acceptor properties.

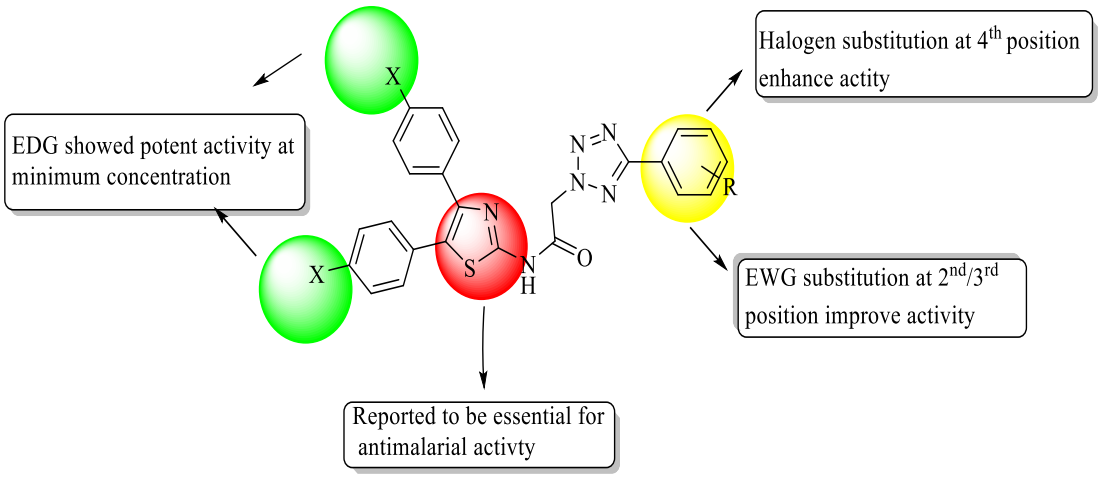


**Fig. 4.6** SAR analysis of the synthesized compounds (**186-224**) highlighting key pharmacophoric regions

Conversely, 3-chlorophenyl substitution (**188**) leads to a complete loss of activity, indicating that the chlorine atom's position is critical. This suggests that steric hindrance or electronic effects at the 3-position disrupt essential molecular interactions. In contrast, 4-chlorophenyl substitutions (**193, 206**) showed moderate activity, implying that chlorine at this position is more favourable.

❖ **Influence of nitro groups**

The introduction of nitro groups results in variable effects depending on their position. 3-Nitrophenyl (**190**) and 2-nitrophenyl (**195**) substitutions exhibit enhanced potency, suggesting that electron-withdrawing effects at these positions promote stronger receptor interactions. However, nitro substitutions at other positions (**189, 202**) showed weaker activity, indicating positional selectivity in binding affinity.

❖ **Hydroxyl and methoxy groups**

The presence of hydroxyl and methoxy groups generally correlates with reduced activity. 3-Hydroxyphenyl (**186**) and 3-methoxyphenyl (**194**) substitutions showed lower potency, likely due to increased hydrogen bonding with solvent molecules, reducing target affinity. Interestingly, 4-methoxyphenyl (**187**) displays moderate activity, indicating that methoxy at this position maintains some binding potential, possibly through favourable electronic effects.

❖ **Effect of alkyl groups**

Alkyl-substituted derivatives exhibited varied activity, with *p*-tolyl (**191**) outperforming *m*-tolyl (**193**), suggesting that steric effects influence receptor binding. The isopropyl-substituted compound (**197**) maintains moderate potency, likely due to hydrophobic interactions enhancing stability within the binding site.

**Conclusion**

This refined SAR analysis highlights key structural modifications influencing bioactivity:

- Bromine and fluorine substitutions found to enhance activity, particularly at the $4^{th}$ and $3^{th}$ positions.
- Chlorine substitution is position-dependent, with 4-chlorophenyl maintaining moderate activity while 3-chlorophenyl results in complete loss.
- Nitro groups at the $3^{rd}$ and $2^{nd}$ positions improved activity due to electron-withdrawing effects.
- Hydroxyl and methoxy groups generally reduce activity, except for 4-methoxyphenyl, which showed moderate potency.
- Alkyl groups demonstrate variable effects, with *p*-tolyl performing better than *m*-tolyl, due to steric considerations.

These findings establish a framework for further structural optimizations of tetrazolyl-thiazole derivatives, emphasizing halogenation and electron-withdrawing modifications to enhance potency.

From the biological data structure activity relationship of the synthesized compounds (**263-275** and **288-297)** has been concluded. We are having two core structure compounds:

- Isoindoline-1,3-dione-based chalcones
- N-Benzylpiperidine-4-carboxamide derivatives

**SAR studies of isoindoline-1,3-dione-based chalcones (263-275)**

Effect of substituents on the chalcone core (isoindoline-1,3-dione derivatives)

❖ **Fluorophenyl substituents** (**270- 275**)

Compound (**270, 272, 273)** showed high activity at 10µM but reduced significantly at 500nM and 50nM.Fluorine at the para position in compound (**272, 273**) contributes to enhanced lipophilicity, leading to increased cell permeability. Compound (**273)** (bis-fluorophenyl chalcone) retained higher activity at 500nM, indicating

fluorine's role in maintaining potency.

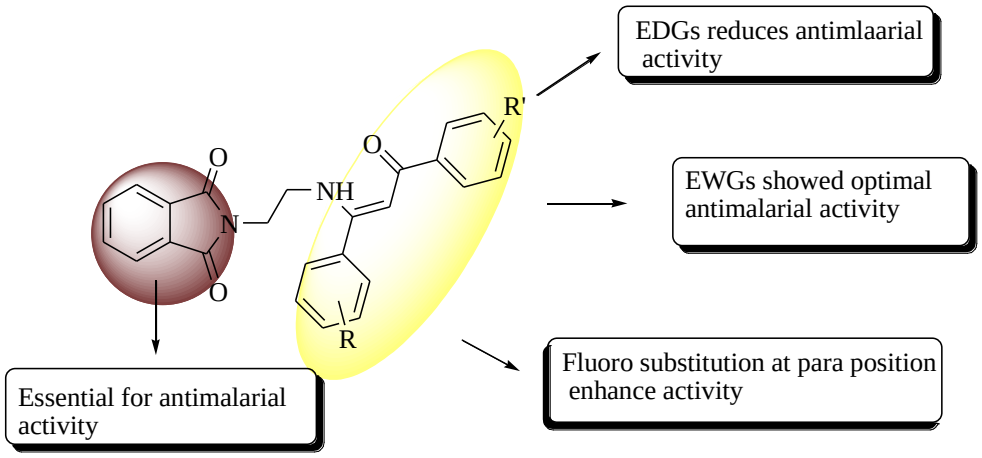


**Fig. 4.6** SAR analysis of the synthesized compounds (**263-275**) highlighting key pharmacophoric regions

- **Hydroxyphenyl and aminophenyl derivatives** (**266-269**)

These compounds exhibited no or minimal response at all concentrations. The hydroxyl (-OH) and amino (-$NH_2$) groups might lead to hydrogen bonding interactions that reduce lipophilicity, thus affecting cell permeability. Compound (**267** and **269**) (hydroxy/bromo substitutions) had no activity, suggesting that electron-donating groups may reduce binding affinity.

- **Bromo- and nitro-substituted chalcones** (**271, 275**)

Compound (**271** and **275)**, which contain nitro and halogen substituents, showed poor activity across concentrations. Nitro at meta/para positions may influence electronic distribution, leading to reduced receptor interaction. Bromine at meta-position (**269**) further diminishes activity, possibly due to steric hindrance.

**SAR studies of *N*-benzylpiperidine-4-carboxamide derivatives (288-297)**

Effect of substituents on the *N*-benzylpiperidine-4-carboxamide derivatives as discussed in **(Fig. 4.8**).

- **Most potent compounds** (**290, 291, 293, 294**)

Compound (**294)** (3-chlorobenzyl derivative) retained high activity at 10µM, 500nM, and even 50nM, indicating strong receptor interaction. Compound (**288, 291,** and **293)** also showed sustained activity, likely due to trifluoromethyl (-$CF_3$), nitro (-$NO_2$), and methoxy (-$OCH_3$) groups, which enhance electronic interactions and bioavailability. The methoxy (**293**) and difluoro (**295**) groups seem to stabilize activity

across concentrations.

❖ **Moderately active compounds** (**296, 297**)

Compound (**296)** (*p*-fluorobenzyl) and (**297)** (*p*-chlorobenzyl) showed moderate responses, indicating that halogen substitution on benzyl rings influences receptor affinity. These compounds exhibit some loss of activity at lower concentrations, but retain moderate binding potential.

❖ **Inactive or weakly active compounds** (**288, 289**)

Compound **(288)** and (**289)** exhibited little to no response, suggesting that electron-withdrawing groups in the benzyl moiety (such as nitro or hydroxyl) might disrupt receptor binding.

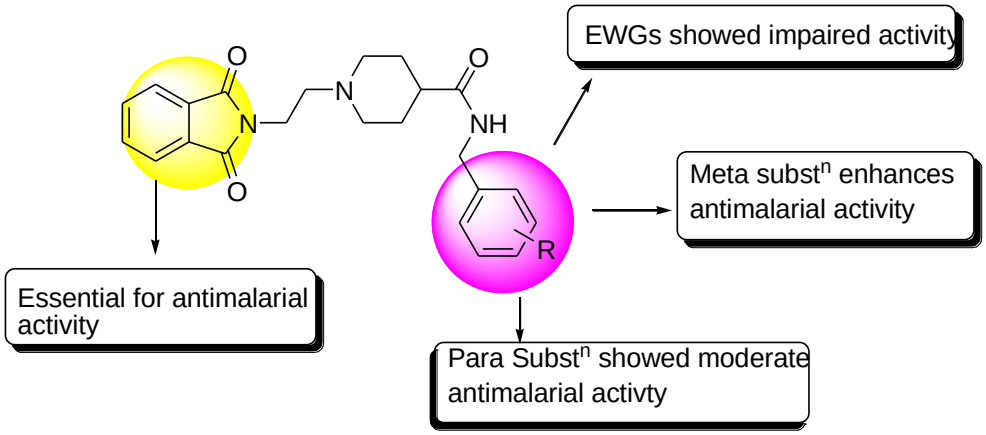


**Fig. 4.6** SAR analysis of the synthesized compounds (**288-297**) highlighting key pharmacophoric regions

Overall, the SAR analysis suggests that fluorinated chalcones, particularly bis-fluorophenyl derivatives, exhibit superior activity due to enhanced lipophilicity and cellular uptake. Electron-withdrawing groups such as nitro and bromine tend to diminish biological activity, possibly due to steric or electronic interference. Among piperidine derivatives, the presence of trifluoromethyl, methoxy, and chlorobenzyl groups appears to significantly improve potency and receptor binding, making these compounds promising candidates for further optimization. Future structural modifications should focus on enhancing lipophilicity and optimizing halogen placement to improve biological activity and selectivity.

**References**

(1) Saikia, L.; Baruah, J. M.; Thakur, A. J. A Rapid, Convenient, Solventless Green Approach for the Synthesis of Oximes Using Grindstone Chemistry. *Organic and Medicinal Chemistry Letters* **2011**, *1* (1), 12.

(2) Xia, J.-J.; Wang, G.-W. Efficient Preparation of Aldoximes from Arylaldehydes, Ethylenediamine and Oxone in Water. *Molecules (Basel, Switzerland)* **2007**, *12* (2), 231–236.

(3) Barmade, M. A.; Agrawal, P.; Rajput, S. R.; Murumkar, P. R.; Rana, B.; Sahal, D.; Yadav, M. R. Novel Quinolinepiperazinyl-Aryltetrazoles Targeting the Blood Stage of Plasmodium Falciparum. *RSC Medicinal Chemistry* **2024**, *15* (2), 572–594.

(4) Tamami, B.; R. Kiasat, A. Dehydration of Aldoximes to Nitriles Using a Polymeric Reagent. *J. Chem. Res. (S)* **1999**, No. 7, 444–445.

(5) Yang, S. H.; Chang, S. Highly Efficient and Catalytic Conversion of Aldoximes to Nitriles. *Organic Letters* **2001**, *3* (26), 4209–4211.

(6) Kazemi, F.; Kiasat, A. R.; Javeherian, M. Improved and Efficient Conversion of Nitriles Using $Na_2CO_3/SOCl_2$. *ChemInform* **2005**, *37*.

(7) Chaudhari, S. S.; Akamanchi, K. G. Thionyl Chloride-Benzotriazole: An Efficient System For Transformation Of Aldoximes to Nitriles. *Synthetic Communications* **1999**, *29* (10), 1741–1745.

(8) Roh, J.; Vávrová, K.; Hrabálek, A. Synthesis and Functionalization of 5-Substituted Tetrazoles. *ChemInform* **2013**, *44*.

(9) Aminimanesh, A.; Shirian, S. Synthesis of 5-Substituted Tetrazoles from Nitriles Catalyzed by Sulfamic Acid. *Organic Preparations and Procedures International* **2017**, *49* (4), 346–354.

(10) Nagaraju, K.; Lalitha, G.; Singh, P.; Rao, C. V. One-Pot Synthesis of 1-Substituted 1H-1,2,3,4-Tetrazoles from 2aminothiazoles Using Tributylmethylammonium Chloride as a Catalyst. *Heterocyclic Communications* **2017**, *23*, 365–368.

(11) Akhlaghinia, B.; Rezazadeh, S. A Novel Approach for the Synthesis of 5-

Substituted-1H-Tetrazoles. *Journal of the Brazilian Chemical Society* **2012**, *23*, 2197–2203.

(12) Jin, T.; Kitahara, F.; Kamijo, S.; Yamamoto, Y. Copper-Catalyzed Synthesis of 5-Substituted 1H-Tetrazoles via the [3+2] Cycloaddition of Nitriles and Trimethylsilyl Azide. *Tetrahedron Letters* **2008**, *49* (17), 2824–2827.

(13) Li, G.; Shao, K.; Umeshappa, C. S. Recent Progress in Blood-Brain Barrier Transportation Research. In *Brain Targeted Drug Delivery System*; Gao, H., Gao, X., Eds.; Academic Press: 2019; pp 33–51. ISBN 9780128140017.

(14) Daina, A.; Michielin, O.; Zoete, V. SwissADME: A Free Web Tool to Evaluate Pharmacokinetics, Drug-Likeness and Medicinal Chemistry Friendliness of Small Molecules. *Scientific Reports* **2017**, *7*, 42717.

(15) Veber, D. F.; Johnson, S. R.; Cheng, H. Y.; Smith, B. R.; Ward, K. W.; Kopple, K. D. Molecular Properties That Influence the Oral Bioavailability of Drug Candidates. *Journal of Medicinal Chemistry* **2002**, *45* (12), 2615–2623.

(16) Barmade, M. A.; Agrawal, P.; Rajput, S. R.; Murumkar, P. R.; Rana, B.; Sahal, D.; Yadav, M. R. Novel Quinolinepiperazinyl-Aryltetrazoles Targeting the Blood Stage of Plasmodium Falciparum. *RSC Medicinal Chemistry* **2023**, *15*, 572–594.

(17) Baniecki, M. L.; Wirth, D. F.; Clardy, J. High-Throughput Plasmodium Falciparum Growth Assay for Malaria Drug Discovery. *Antimicrobial Agents and Chemotherapy* **2007**, *51* (2), 716–723.